doi:10.26443/seismica.v5i2.2806

Seismic noise and data quality of broadband stations of the Alaska Geophysical Network

Heather McFarlin *[1], **Natalia A. Ruppert**[2], **Austin Holland**[1]

[1]Alaska Earthquake Center, Geophysical Institute, University of Alaska Fairbanks, Fairbanks, AK, USA, [2]USGS Earthquake Science Center, Seattle, WA, USA

Author contributions: *Conceptualization*: H. McFarlin, N. Ruppert. *Data Curation*: H. McFarlin. *Formal Analysis*: H. McFarlin, N. Ruppert. *Funding Acquisition*: N. Ruppert, A. Holland. *Investigation*: H. McFarlin, N. Ruppert. *Methodology*: H. McFarlin, N. Ruppert. *Project Administration*: N. Ruppert, A. Holland. *Resources*: H. McFarlin, N. Ruppert. *Software*: H. McFarlin. *Supervision*: N. Ruppert, A. Holland. *Validation*: H. McFarlin, N. Ruppert, A. Holland. *Visualization*: H. McFarlin, N. Ruppert. *Writing – original draft*: H. McFarlin, N. Ruppert. *Writing – review & editing*: H. McFarlin, N. Ruppert, A. Holland.

Abstract The Alaska Earthquake Center operates the Alaska Geophysical Network (AGN), a statewide array of more than 250 geophysical stations spanning diverse and extreme environments. Maintaining continuous, high-quality seismic observations requires systematic evaluation of station performance in remote locations. We assess background seismic noise and broadband sensor stability across the AGN from January 2021 through December 2024 using probabilistic power spectral density analyses across six period bands, while sensor stability is evaluated using mass recentering records. Noise levels vary substantially across the network. Coastal, island, and Aleutian Arc stations exhibit elevated microseism-band noise, whereas the quietest stations occur in Interior and northern Alaska. Steel-cased boreholes in competent bedrock show the lowest noise and most stable performance, while stations in sediments, organic soils, or shallow vaults exhibit higher noise and variability. Seasonal microseism increases reflect ocean wave activity, while long-period noise and mass recentering patterns indicate freeze-thaw and ground deformation effects. Combining noise metrics with mass recentering identifies stations at elevated risk of degradation. These datasets provide independent indicators of site stability and improve station health assessments. Results show how installation type, geology, and environmental forcing influence long-term performance and support maintenance prioritization, station siting, and network optimization in extreme environments.

Production Editor:
Yen Joe Tan
Handling Editor:
Jonathan Weiss
Copy & Layout Editor:
Théa Ragon

Received:
March 6, 2026
Accepted:
November 10, 2026
Published:
November 24, 2026

1 Introduction

Seismic sensors are designed to record ground motions at a wide range of frequencies and amplitudes; the broadband seismic data exhibit continuous background noise rather than a zero-amplitude baseline. In addition to earthquakes, the records contain signals from environmental factors (winds, rivers, oceans/microseisms, magnetic field variations), human activities (construction, traffic, mechanical devices at nearby structures, foot traffic), and instrument self-noise (e.g., Peterson, 1993; McNamara and Buland, 2004; Aderhold et al., 2015; Hutt et al., 2017; Busby et al., 2018; Dybing et al., 2019; Johnson et al., 2019; Anthony et al., 2022; Ringler et al., 2024). Ground conditions also influence seismic wavefields (Peterson, 1993), such as amplifications caused by sediments, from large-scale effects in sedimentary basins to smaller-scale site effects from soft sediments or soil. Additionally, Alaska experiences seasonal variations in nearly all the above factors (environmental, human activities, ground conditions), compounding any noise experienced by a sensor. The main function of a regional seismic monitoring network is to provide high-quality data for earthquake monitoring. By understanding the noise characteristics of a seismic station, we can inform recommendations for designing and maintaining site infrastructure that results in the best possible data quality.

The Alaska Geophysical Network (AGN) is operated and maintained by the Alaska Earthquake Center (AEC, 1987). As of 2024, it consisted of 254 seismic stations (Figure 1). Some sites date back to the early 1970s, installed in the wake of the 1964 Great Alaska Earthquake, while others are more recent acquisitions (Ruppert & West, 2020). Specifically, 96 of these sites were adopted from the EarthScope US Transportable Array project between 2019 and 2021 (Freymueller and West, 2024; Busby and Aderhold, 2020; Ruppert and West, 2019). These adoptions significantly expanded the AGN footprint, improving spatial coverage and lowering detection thresholds in regions of Alaska that previously had sparse broadband instrumentation.

Alaska's seismic network operates across a wide range of climatic and geologic environments, many of which are characterized by extreme weather, difficult terrain, and limited infrastructure. These conditions significantly constrain physical access to seismic stations, with site visits often not feasible during winter months due to personnel safety concerns and logistical barriers associated with remote travel. Even during summer months, access to many stations remains logis-

*Corresponding author: hlmcfarlin@alaska.edu

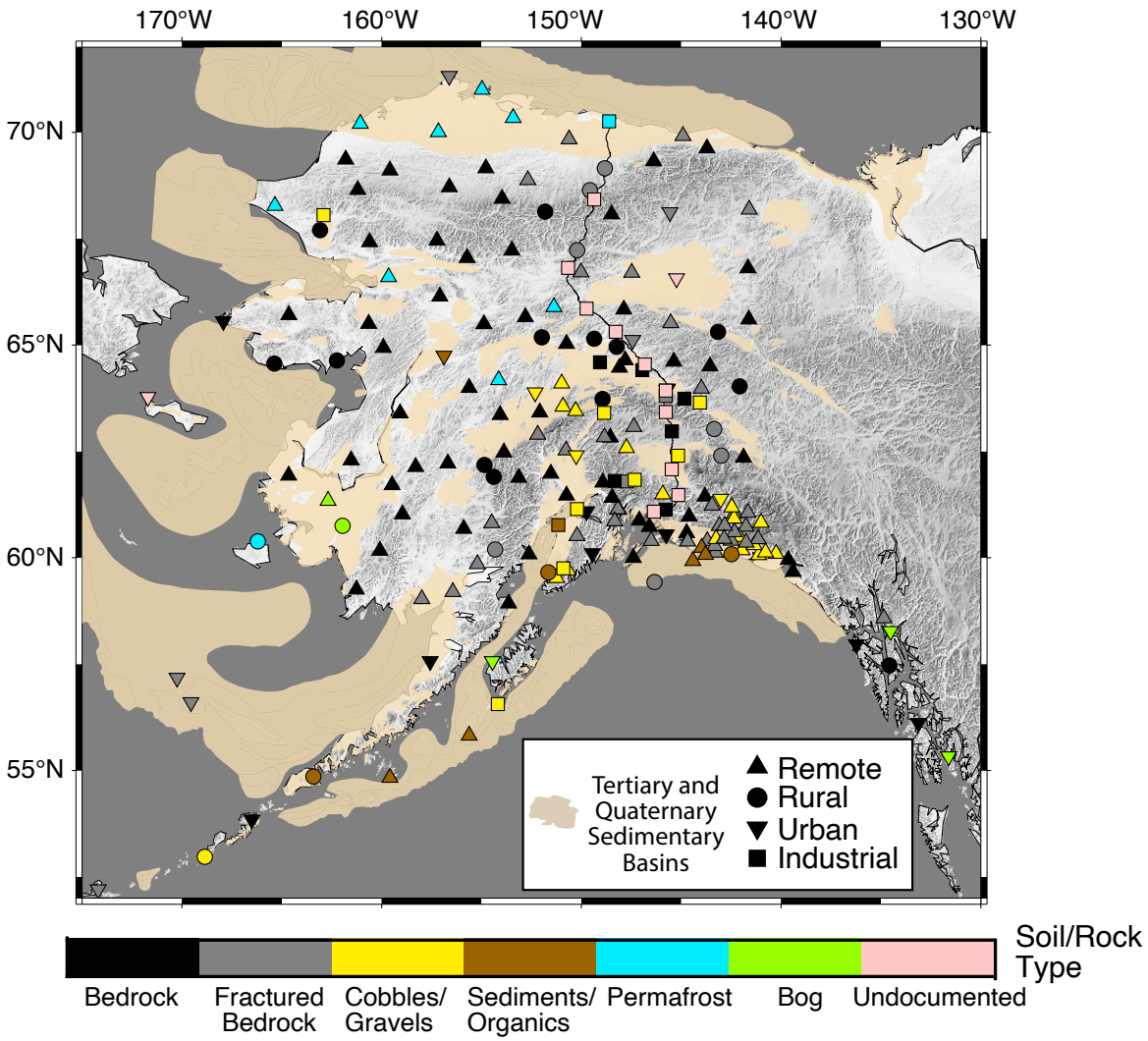

Figure 1 Locations of broadband stations with network code AK operational in 2024. Different symbols represent the remoteness index, with colors indicating soil and rock conditions at the sensor placement depth. Beige polygons indicate Quaternary and Tertiary sedimentary basins mapped by the U.S. Geological Survey (Kirschner, 1988).

tically challenging and costly because travel frequently requires helicopters or small aircraft. As a result, routine station maintenance and troubleshooting cannot rely on frequent field visits and must instead be supported through robust remote monitoring strategies. Effective remote data quality control supports identification and diagnosis of issues such as timing errors, sensor degradation, telemetry failures, or environmentally driven noise changes, allowing the limited field resources to be prioritized and deployed only when necessary.

Many newly adopted seismic stations are in areas of permafrost, where freeze-thaw cycles in the active layer, as well as local permafrost degradation, some caused by the sensors themselves, increasingly impact station stability and data quality. These effects have become more pronounced in recent decades as permafrost thaws at faster rates than observed over the past forty years (United States Environmental Protection Agency, 2022; Smith et al., 2022). In addition to environmental drivers, data quality at some sites is increasingly affected by human activity and animal interactions at locations that were previously undisturbed. Accurately distinguishing among environmental, anthropogenic, biological, and instrumental noise sources is therefore essential for effective remote diagnosis and informed operational decision-making. This distinction is achieved through integrated analysis of seismic waveforms, mass position time series, and probabilistic power spectral density estimates, complemented by site photos and field notes that provide critical context. Together, these tools support efficient planning of targeted site visits and enable near-real-time identification of anomalous events, such as sudden noise increases associated with wildlife interactions, explosions (mining, bolides, aircraft, etc.), aircraft activity, or other events that may affect station performance.

A few studies have examined the noise characteristics of seismic stations in Alaska in detail. D'Alessandro and Ruppert (2012) analyzed noise characteristics of the Alaska regional seismic network in terms of earthquake detection capabilities. Tsai and McNamara (2011) evaluated data from three seismic sites bordering the Bering Sea to quantify the influence of sea ice on ocean-generated noise. Smith and Tape (2019a) studied the noise behavior of 16 seismic stations in central Alaska,

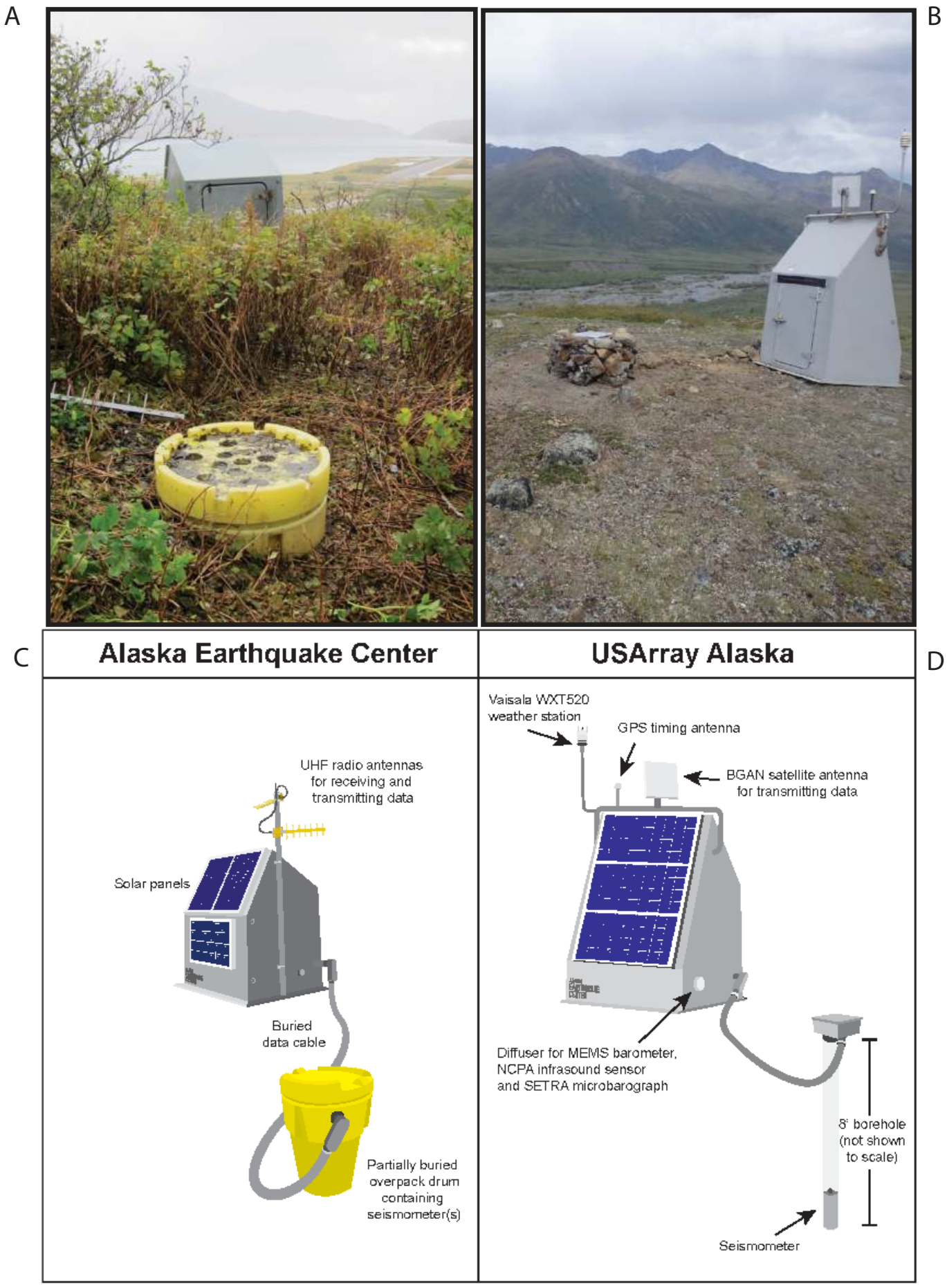

Figure 2 Photos and schematics of typical sites installed in the Alaska Geophysical Network. A) FALS, the noisiest site; B) E24K: the overall quietest site; C) schematics of a typical AEC-style vault; and D) schematics of a typical Alaska TA-style borehole.

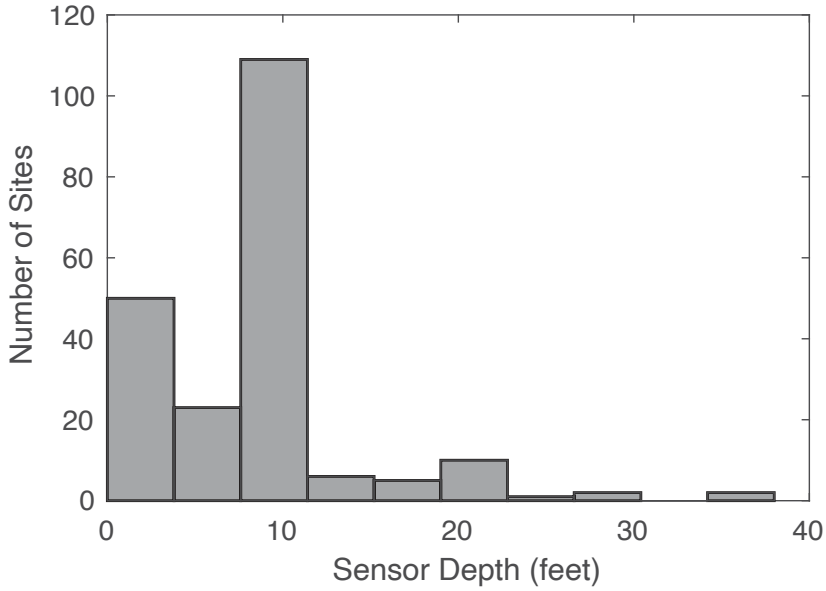

Figure 3 Distribution of sensor placement depths. The majority of sensors are less than 10 feet deep. The two largest groups are TA-style boreholes (8-9 feet deep) and AEC-style shallow vaults (2-4 feet deep).

primarily from a temporary deployment, to document the influence of rivers, wind, and sedimentary basins. Smith and Tape (2019b) documented how the Cook Inlet basin affects the seismic wavefield and the noise behavior of 28 seismic stations in and around south-central Alaska. Continuing work on the response of basins to the seismic wavefield, Smith et al. (2022) studied Nenana basin in Interior Alaska, further documenting amplification of seismic waves and ambient noise. (Quigley and West, 2023) focused on 110 stations, all with collocated wind sensors, in the Alaska component of the US Transportable Array project and documented the influence of wind on seismic noise spectra.

The most comprehensive assessment of background seismic noise in Alaska and western Canada, to date, was conducted by Ringler et al. (2024), who analyzed newly adopted US Transportable Array sites; however, this work did not include backbone AK stations. Our study complements and extends this analysis by evaluating noise levels and data quality across the entire AGN, including both adopted US Transportable Array and backbone AK sites that were active through December 2024, while providing local context to investigate potential noise sources. We conducted a network-wide assessment of broadband data quality using a combination of background noise characteristics and sensor mass position behavior to identify regional patterns, station-specific outliers, and indicators of chronic instability.

Background seismic noise was quantified using probability power spectral density (PPSD)-derived noise level estimates (specifically, modal noise levels following McNamara and Buland, 2004) computed for each broadband channel at discrete frequencies and times, as provided by the EarthScope Modular Utility for Statistical Knowledge Gathering (MUSTANG) system (Casey et al., 2018). Analysis of these noise characteristics enabled identification of spatially coherent noise features as well as anomalous stations requiring further investigation. Because seismic wavefields are three-dimensional, accurate ground-motion recording depends on properly functioning and well-leveled three-component sensors, and deviations in sensor orientation or component damage can directly affect data quality. To evaluate sensor stability, we analyzed internally sourced state-of-health (SOH) information, focusing on mass position behavior and recentering performance, which may be influenced by environmental factors such as temperature variations, sensor tilt, or changes in pore pressure. Collectively, these complementary noise and mass analyses support the identification of chronic instability issues and provide insight into the causes of seasonal and site-specific noise at stations across the network.

This study presents a comprehensive, network-wide assessment of broadband seismic data quality across the Alaska Geophysical Network, integrating background noise analysis with sensor state-of-health diagnostics. The results characterize data quality across diverse environmental settings and demonstrate a practical, transferable framework for evaluating and maintaining large seismic networks operating in remote and environmentally challenging regions.

2 Data

As of late 2024, 206 of the 254 AGN sites had free-field broadband sensors with high-gain channels (Figure 1). The field sites include several infrastructure components (Figure 2). A typical remote site has a fiberglass hut with a footprint of about 5 by 5 ft and a height of 5 to 6 ft, depending on the design. The inside of the hut contains a power system (a combination of lead-acid, lithium, or celair batteries), data loggers, and communication devices, while solar panels, communication antennas, and other devices are externally mounted. Seismic sensors are located at least 3 ft away from the hut and, in many cases, several feet away (average TA-

adopted site is about 15 ft distance, and best practice is for the sensor housing-hut distance to be twice the height of the hut; there are limitations to this distance that are site specific and are due to the site conditions). Sensor housing varies across the network, with most installations consisting of boreholes of varying depths, either steel- or PVC-cased, with inner diameters ranging from 8 to 12 inches, or shallow hand-dug insulated heavy-duty PVC vaults (Figure 3). Many boreholes were inherited from the US Transportable Array, although some date back to the 1970s, and 15 AGN backbone sites have been converted to boreholes since 2018. Borehole depths range from 5 to 38 ft, with most sites at depths of 10 ft or less (Figure 3). The deepest borehole is located at site PAX, originally installed in the 1970s and upgraded with a new sensor by the US Transportable Array project. Emplacement depth can influence seismic noise, with deeper installations generally providing greater attenuation of near-surface noise sources, particularly at higher frequencies (Hutt et al., 2017). The predominance of shallow boreholes in the AGN therefore provides important context for interpreting network-wide noise performance and recognizing that emplacement depth may contribute to observed noise differences alongside installation type and other site characteristics; however, a quantitative assessment of depth versus noise performance is beyond the scope of this study. Additional installation types include directbury (BAT, CYK) and TA-style large vaults (ATKA, POKR) (Table S1). One site (BAL) has an uninsulated metal culvert installed in the 1970's; while classified as a vault-type installation, this site experiences pronounced diurnal temperature fluctuations. All other vaults are constructed of PVC and do not experience these fluctuations.

The AGN utilizes a diverse set of broadband sensors, including Nanometrics Trillium 120-second Posthole, Trillium 120, and Trillium 240 instruments, Streckeisen STS-2, STS-4B, and STS-5A sensors, and Güralp CMG3T-120 second, CGM3ESP-30 and -60 second, and CMG40T-30 second sensors (Table S1, Table S2 "Site Information" sheet). During the analysis period from January 2021 through December 2024, digitization was primarily performed using Kinemetrics Quanterra 330 (Q330) with several Q8 units and two Nanometrics Centaur digitizers. Typical sampling rates for broadband channels were 50 samples per second (sps), with three stations recording at 100 sps.

Several stations or collocated broadband sensors were excluded from the dataset due to data availability. Sites DCPH and H23K did not have sufficient continuous data for any year between 2021 and 2024 (Table S2, "Availability" Sheet) and were therefore retained only for completeness in station listings but excluded from quantitative analyses. Stations TOLK, POKR, and WRH each operated two collocated broadband sensors, distinguished by differing location codes (e.g., no location code versus 01, or 00 and 01), until 2023. For consistency across the network, only one broadband sensor per site was selected for analysis and visualization.

The seismic waveform data are archived locally at the Alaska Earthquake Center and are also distributed through the EarthScope Consortium Data Management Center (DMC). For stations available at the DMC, EarthScope provides a suite of precomputed data quality metrics via the MUSTANG system (Casey et al., 2018). For this study, we obtained the PPSD-based summary noise level estimates for multiple period bands from the MUSTANG Noise Time Series service (Casey et al., 2018), covering the interval from 2021 through 2024. In addition to these noise metrics, internally generated SOH records documenting sensor mass position and recentering behavior were available for AGN stations, including datalogger logs documenting mass recentering commands. These SOH records include the command type, execution time, and station identifier, and provide a network-wide record of mass recentering activity over the same time period (Table S3).

During the 2021-2024 analysis period, some stations underwent instrumentation changes related to data quality or availability issues. These changes primarily included sensor replacements due to malfunctioning broadband instruments, as well as sensor cable replacements and digitizer swaps resulting from clock instability, repeated reboots, or other operational failures. Such changes introduce potential variability in data characteristics over time. All known instrumentation changes during the study period are documented in Table S2 ("Site Information" sheet). Together, the resulting noise and mass position datasets provide the observational basis for the analyses of background noise characteristics and sensor stability described below.

3 Methods

3.1 PPSD-Based Noise Analysis

To consistently and robustly characterize seismic station noise, we apply the probability power spectral density (PPSD) method of McNamara and Buland (2004). A PPSD represents the distribution of noise power over time at each frequency, while the statistically most probable noise power at a given frequency is summarized as the PPSD mode value (Figure 4). This approach provides a standardized quantitative measure of typical station noise behavior suitable for network-wide analysis.

The computation of PPSD mode values, as implemented in the EarthScope MUSTANG system (Casey et al., 2018), begins by reading raw waveform time series in digital counts into a processing buffer. The data are windowed into 1-hour segments with ½-hour overlap, transformed to the frequency domain, and stacked to generate power spectral density (PSD) estimates. Instrument response information is then applied to convert the PSDs from counts to physical ground-motion units. The resulting 1-hour PSDs are subsequently used to calculate daily PPSD mode values at the selected frequencies (Casey et al., 2018). Although initial waveform data are in digital counts, the final PPSD mode values are expressed in physical ground-motion units (typically velocity squared per Hz) after instrument correction and may be converted to decibels (dB) for visualization.

We evaluated PPSD mode values across six nominal

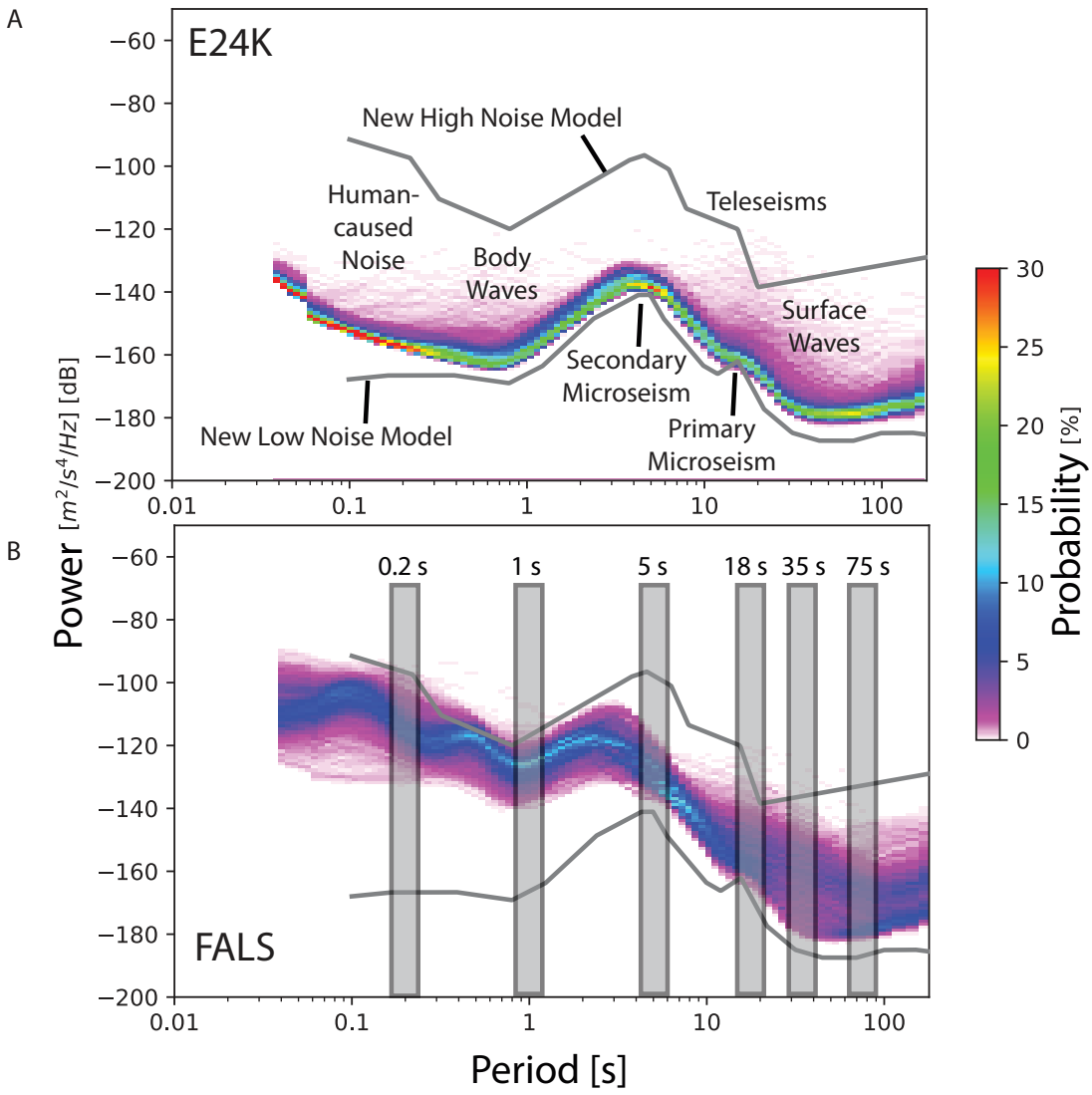

Figure 4 Annotated PPSD examples of AK sites (A) E24K (overall quietest site) and (B) FALS (noisiest site). Both PPSD plots are for the vertical channels of each station. Black lines are the Peterson New High and New Low Noise Models (Peterson, 1993). A) Station E24K PPSD plot annotated to show the expression of various features of seismic data. Data is from June 6 to August 17, 2021. B) Station FALS annotated to show the period bands used in this study. Data is from May 31 to August 11, 2023.

period bands representing distinct noise regimes: 0.2s (anthropogenic noise), 1.0s (teleseismic body waves), 5.0s (secondary microseism), 18.0s (primary microseism), 35.0s (long-period surface waves), and 75.0s (also long-period surface waves). For each nominal period, MUSTANG selects the precomputed frequency closest to the requested value; consequently, the frequency represented by a nominal period may differ slightly from the mathematical inverse (Casey et al., 2018). These period bands were selected following Anthony et al. (2022) and Ringler et al. (2024), to facilitate comparison with established definitions of typical noise regimes (Peterson, 1993; Berger et al., 2004). The underlying PPSD computation follows the McNamara and Buland (2004) method, which John and West (2024) demonstrated is well-suited for large-scale broadband network assessments, making it appropriate for this network-wide evaluation of AGN data quality.

Network-wide seismic noise assessments have previously been used to characterize station performance and identify operational issues in large seismic networks. McNamara and Buland (2004) developed the probability-density approach used here to evaluate ambient seismic noise across stations contributing to the U.S. National Seismograph Network and Advanced National Seismic System (ANSS), demonstrating its utility for assessing station performance and detecting operational issues. Berger et al. (2004) similarly characterized ambient noise across stations in the Global Seismograph Network (GSN) and ANSS, highlighting the value of network-wide noise statistics for evaluating station performance. McNamara et al. (2005) further demonstrated the use of probability-density noise analyses for identifying station artifacts and operational issues, including data gaps and mass-recentering behavior. Building on these large-network quality control efforts, this study applies PPSD mode values across the AGN to evaluate spatial, environmental, seasonal, and installation-related controls on station noise.

For each station-channel combination, 2024 PPSD

mode time series were obtained from the EarthScope MUSTANG Noise Time Series service (Casey et al., 2018) and imported into MATLAB© for analysis. Summary statistics, specifically the median and standard deviation for each period band, were calculated for the full analysis year as well as separately for summer (June 1–August 31) and winter (December 1–February 28) to enable seasonal comparisons of noise characteristics. We note that global and regional earthquakes, including aftershock sequences, can transiently elevate seismic noise levels; however, similar to Berger et al. (2004) and McNamara et al. (2005), because the statistics are computed over long time intervals, these episodic signals are not expected to bias the overall noise estimates significantly.

Percent data availability was also evaluated for each station for the full 2024 year and for each season separately. If availability for any time period fell below 50%, PPSD mode data from the preceding year 2023 were incorporated. For a small number of stations with persistent data gaps, data from 2022 or 2021 were used to achieve sufficient coverage (Table S2 "Availability" sheet). Stations with insufficient data coverage across the analyzed years were excluded from the analyses entirely.

3.2 Site classification and metadata

The AGN has a heterogeneous composition in terms of sensor housing, sensor and datalogger types, geographic distribution, and rock conditions. Our analysis includes an examination of noise characteristics with respect to geographic location, remoteness factor, sensor housing, rock/soil conditions at the sensor placement depths, and seasonal variations. We do not attempt to create groupings of similar sensor+datalogger configurations since some groups would be too small to provide statistically meaningful results.

To examine spatial and environmental influences on station noise, each site was categorized according to geographic remoteness, sensor emplacement method, and rock/ground type at the depth of sensor placement. The following remoteness factor classifications follow Smith and Tape (2019a):

Remote: no human activities except for routine field maintenance

Rural: occasional human presence and activities

Urban: daily human presence and activities

Industrial: pipeline pump stations, state microwave sites, tall communication towers, wind farms.

Sensor emplacement classifications are as follows:

Borehole: all depths greater than ~3 ft, PVC- or steel-cased, any diameter (6-12 inches)

Vault (AEC-style): heavy-duty insulated PVC barrels traditionally used by AEC; sensor depth is typically two feet below the surface

Direct-Bury: sensor is buried in the ground and embedded in sand without any casing or enclosure

TA Tank: heavy-duty insulated PVC barrel that is much larger than an AEC-style vault, with a concrete base, and sensor placement is typically five feet below the surface.

Similar to Busby and Aderhold (2020), rock/ground type at sensor depth was classified based on drill logs, field notes, and photos and are as follows:

Bedrock
Fractured Rock
Cobbles and/or gravels
Sediments and/or organics
Permafrost
Bog
Undocumented.

In addition to the classifications described above, stations were also categorized according to whether they are located within mapped sedimentary basins, because basin structure can significantly influence seismic noise characteristics (e.g., Smith and Tape, 2019a, and references therein). Tertiary and Quaternary sedimentary basin boundaries were obtained from Kirschner (1988) and accessed via Alaska Division of Geological and Geophysical Surveys (2020), as shown in Figure 1. Basin polygons were imported into a geographic information system and compared with station coordinates to determine station placement relative to basin boundaries. Stations whose locations fall within mapped basin polygons were classified as basin stations, while stations located outside of these polygons were classified as non-basin stations. Basin classifications for all stations are provided in Table S2 ("Site Information" sheet). Basin depth and internal structural variations were not included in the analysis.

3.3 Mass recenter analysis

To complement the PPSD-based noise analysis and further evaluate sensor stability, we examined mass recentering activity across the network. In addition to thermally induced tilt (Berger et al., 2004), seasonal freeze-thaw cycles and long-term permafrost warming can tilt seismic sensor housings, potentially shifting broadband sensor masses outside of their allowable tilt range and degrading data quality. When sensor masses exceed these limits, ground motions may be poorly recorded or lost entirely, impacting earthquake locations and other analyses (Rohde et al., 2017). If left uncentered, excessive tilt can also physically damage the sensor, sometimes necessitating replacement. Sensor masses that exceed allowable tilt thresholds can also contribute to elevated or anomalous noise levels observed in the PPSD data (Rohde et al., 2017), providing a complementary indicator of station instability. To maintain data quality, sensor masses are periodically recentered, either remotely via datalogger commands or manually during field visits. All recentering commands are logged. (Figure 5A). Frequent recenter events may indicate sensor malfunction, sensor tilt, or movement of the sensor emplacement.

For this study, we evaluated mass recentering activity using sensor-specific tilt thresholds (Table S4). We calculated the number of recenter events for each station over the analysis period and used these counts together with data availability to identify stations with relatively high and low recentering activity. Stations with high data continuity (>80% annual availability) and low

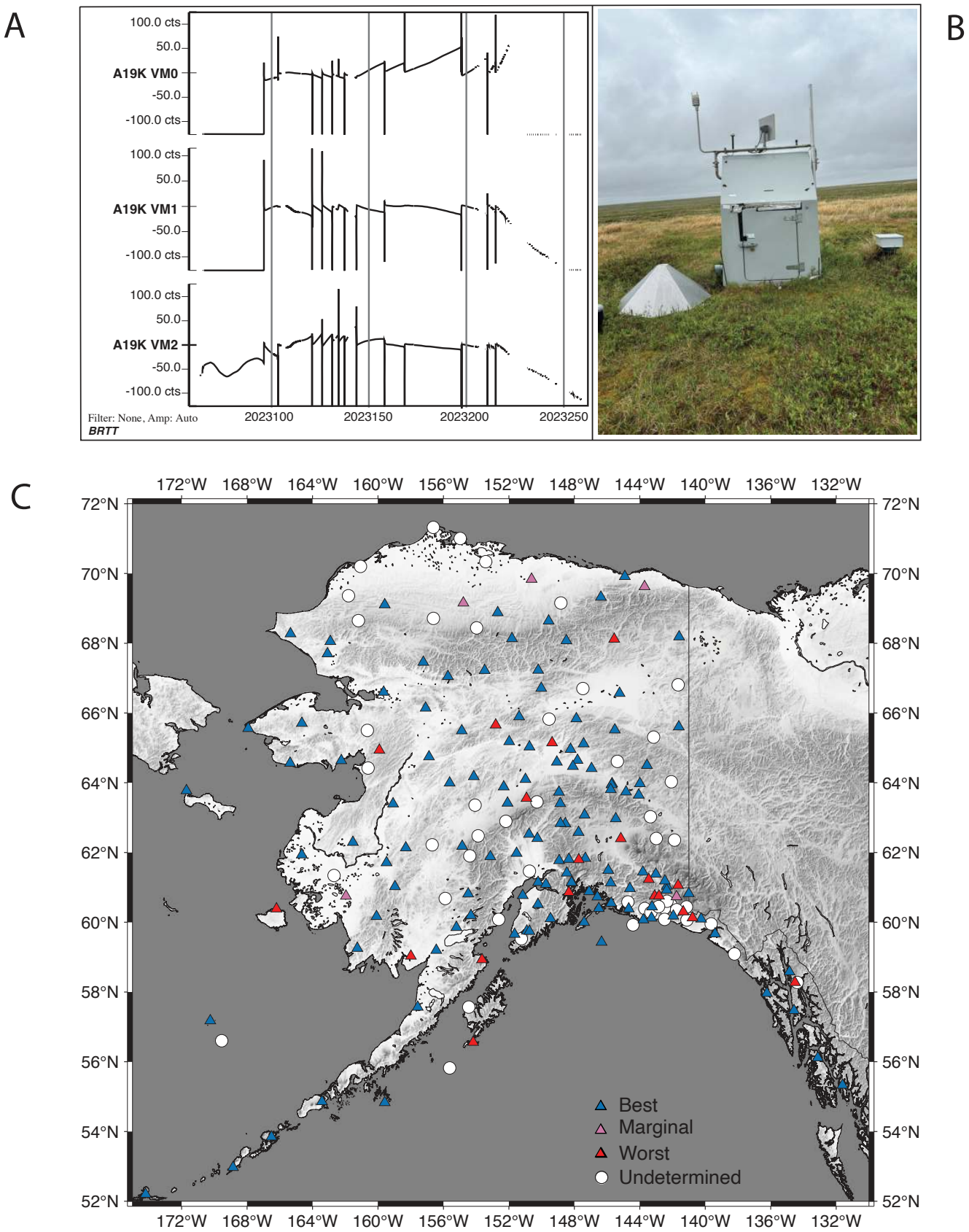

Figure 5 A) Mass position time series for station A19K. Spikes are mass recenters. Gaps are data gaps when the station was out due to telemetry or power issues. B) The photo shows the environment of station A19K in the summer. The drilling log indicates that from 4.6 to 8.8 ft is permafrost and an ice lens. Frequent recenters indicate that the borehole may be subjected to permafrost degradation. The borehole is located near the hut, which may contribute to the instability of the active layer above the permafrost. C) Map of analyzed broadband sites color-coded by assigned performance level for mass recenters. Note that since pipeline sites and sites with Centaurs cannot be recentered, they are excluded from this analysis.

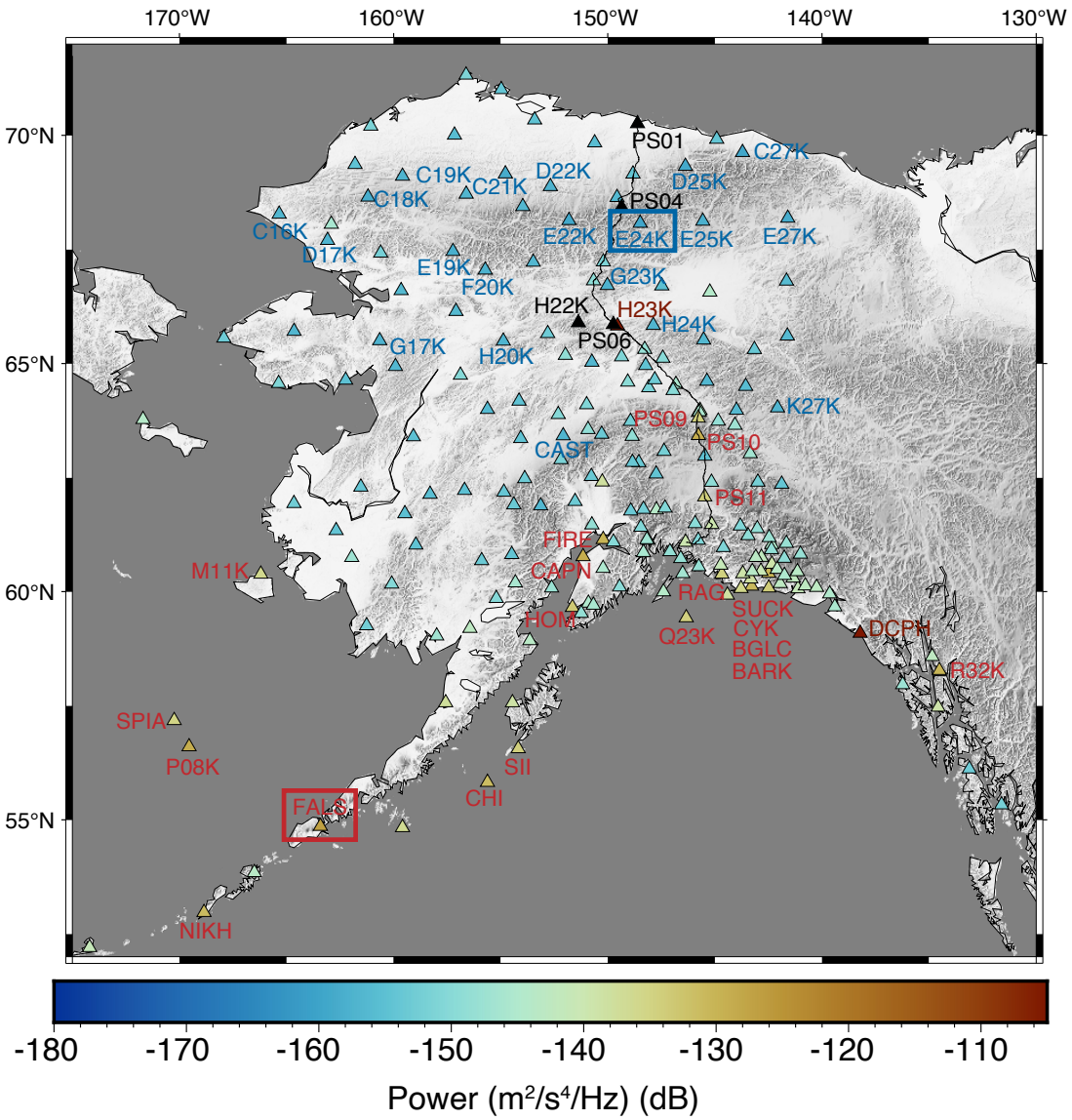

Figure 6 Map of the average of all components and all modes for each station. The 20 quietest and 20 noisiest stations are labeled. The quietest and the noisiest overall stations are E24K and FALS, respectively. The two brown stations are DCPH and H23K, neither of which had enough data to analyze, and thus have noise levels of 0. The black stations were excluded from being categorized as quiet because of known sensor or sensor housing malfunctions.

recenter counts (<12 per year) were designated as the 20 "best-performing." Stations with 50-70% data availability were also classified as "best-performing" when they had six or fewer recenter events, using a proportional reduction in the recenter threshold to account for the shorter observation period. The 20 stations with the highest numbers of recenter events were classified as "worst-performing," while stations with intermediate recentering activity were classified as "marginal-performing". Stations with insufficient data availability to reliably assess recentering behavior were classified as "undetermined" (Figure 5C).

4 Results

4.1 Noise modes analysis

In the following sections, we present results from the PPSD-based noise analysis and mass recentering analysis, examining network-wide trends as well as station-specific outliers across different noise regimes, seasons, and site classifications. Results are structured to first provide a network-wide summary, followed by analyses of period-dependent noise, infrastructure, and environmental influences, and seasonal variations. This organization allows us to move from broad patterns across the AGN to finer-scale behaviors influenced by site characteristics and temporal factors.

For all noise analyses, the two horizontal components were averaged, as they exhibit similar noise levels for the majority of stations and period bands. The vertical component is presented separately to highlight differences in coupling and sensitivity across installations. Unless otherwise noted, classifications of "quietest" and "noisiest" stations are classified based on the average noise levels across all three components. Figures present vertical and horizontal results separately where relevant to facilitate comparison.

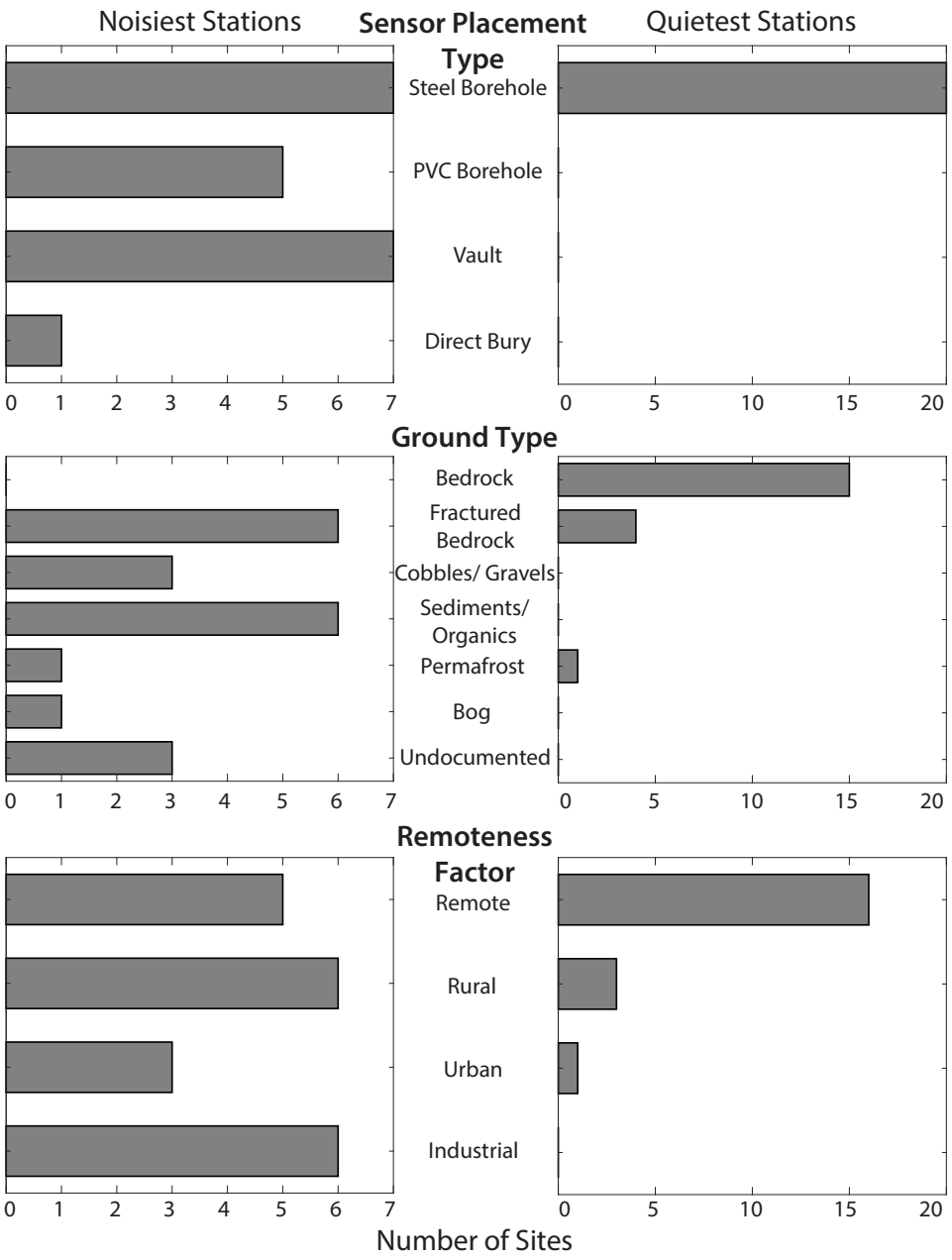

Figure 7 Noisiest (left panels) and quietest (right panels) 10% of all sites grouped by sensor placement type, ground type, and remoteness factor.

4.2 Network-wide average noise analysis

We first summarize network-wide noise characteristics by computing a single annual average for each station across all six period bands and all three components (Figure 6). The quietest site based on annual averages across channels and period bands is H22K, a remote permafrost station with a PVC-cased borehole in Interior Alaska (Figure 6). However, H22K exhibits substantial seasonal variability and documented frost jacking of the borehole casing and is therefore not treated as a representative low-noise benchmark in subsequent analyses. D25K most consistently ranks among the quietest stations, appearing within the lowest 10% of noise levels across all six period bands, while E24K (Figure 4A) is among the quietest 10% in all five of six bands. These results demonstrate that overall annual averages can obscure frequency-dependent station performance. Other stations that rank among the quietest in individual bands, including H21K, PS01, PS04, PS06, and P16K, have documented sensor malfunctions or installation issues and are similarly excluded from discussions as low-noise benchmarks.

The noisiest site overall is FALS, located in a coastal village near the eastern end of the Aleutian Arc with an AEC-style vault embedded in organics-rich, clay-dominated soils (Figure 2A). Among the 10% noisiest stations, six are industrial, three are urban, thirteen are within sedimentary basins, and sixteen are coastal or island stations; more than half are borehole installations and seven are AEC-style vaults. None are in solid bedrock, and only one is on permafrost (Figure 7). BARK is a notable exception to these patterns: despite being a remote AEC-style vault without the dominant environmental or site classifications, it ranks among the noisiest stations. Instrumentation changes at BARK and

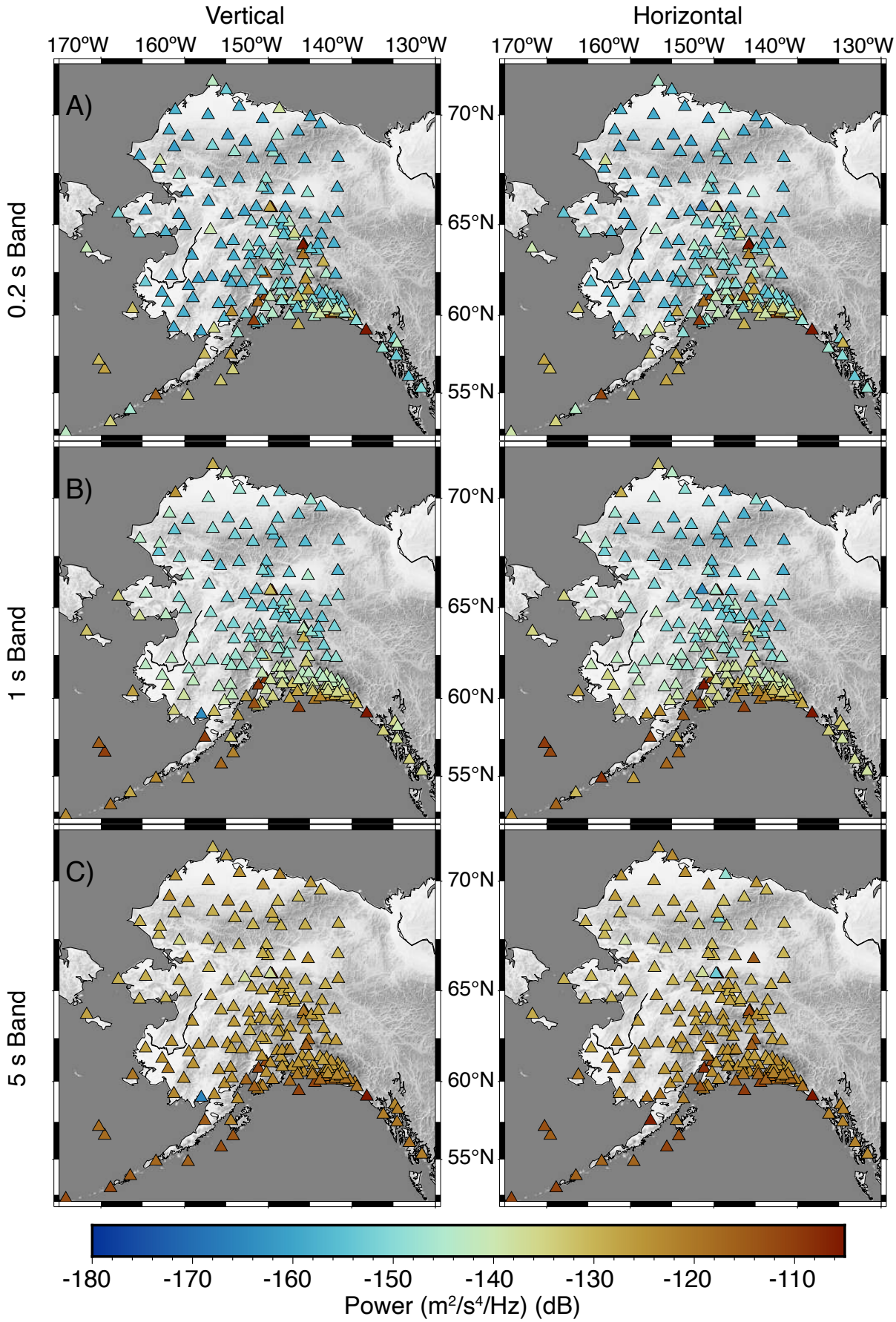

Figure 8 Side-by-side maps of the 6 frequency bands for vertical (left panels) and the average of the two horizontal channels (right panels). The horizontal channel values across all frequency bands are very close to each other, except for a handful of stations discussed in the text. A) 0.2s period band. B) 1s period band. C) 5s period band. D) 18s period band. E) 35s period band. F) 75s period band.

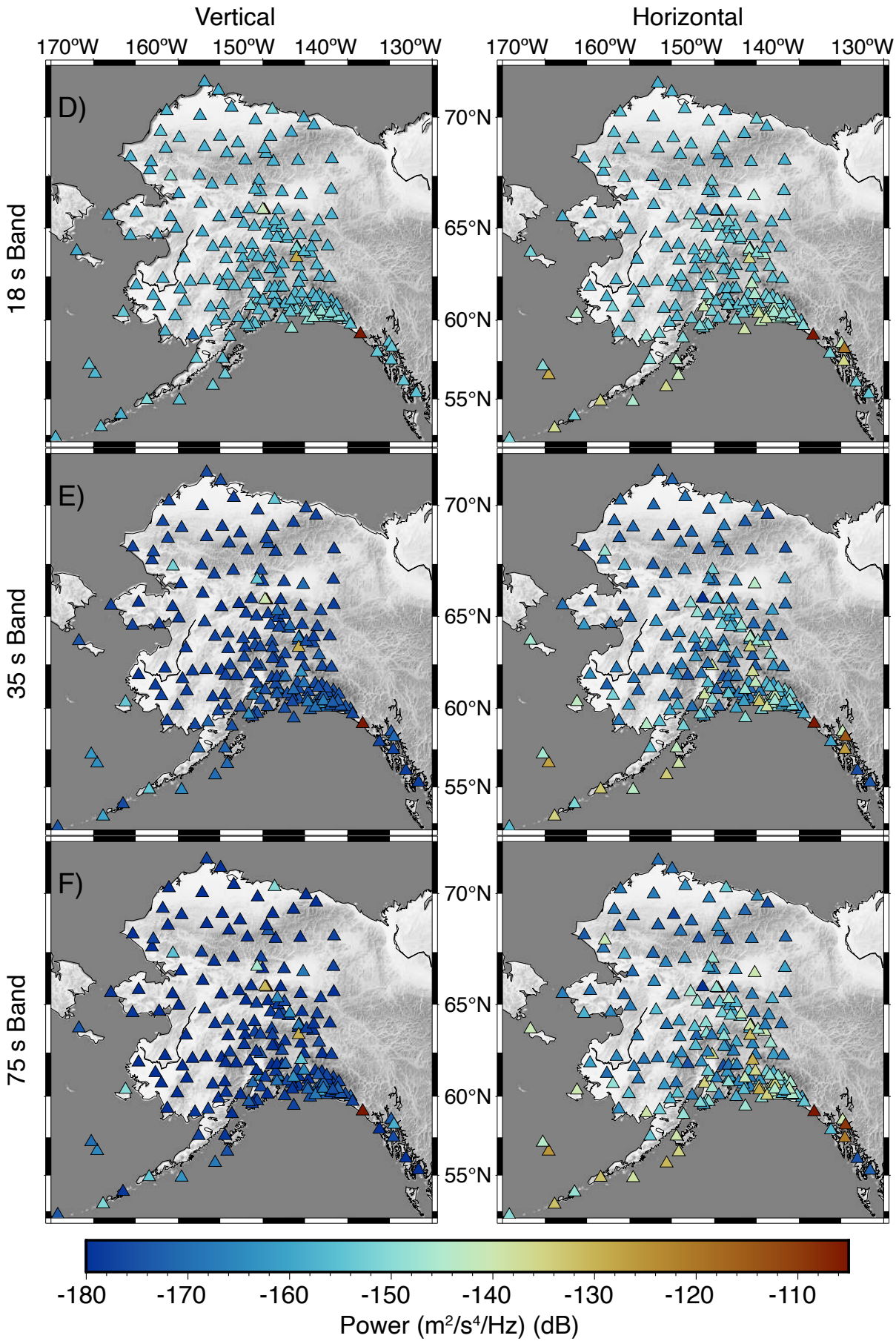

Figure 8 continued

NIKH occurred late in their respective analysis years and therefore had limited influence on their annual averages.

The 10% quietest stations are predominantly remote steel-cased boreholes installed in solid or fractured bedrock, with a small number of rural or urban sites (Figure 7). These network-wide patterns provide a basis for examining how noise varies with period band, sensor emplacement, ground type, and remoteness.

4.3 Noise levels by period band

Noise patterns vary systematically with period band. High-frequency noise is concentrated near anthropogenic and industrial sources, whereas the 5 and 18s bands show strong coastal and ocean-related patterns. At long periods, horizontal noise is highest in southern and coastal Alaska, while the quietest stations across most bands are predominantly remote borehole installations in competent ground.

4.3.1 0.2s period noise characteristics

The 0.2s band is commonly associated with anthropogenic activity and near-surface processes and has also been shown to include contributions from wind-related noise (Dybing et al., 2019; John and West, 2024). Vertical and horizontal components exhibit similar spatial patterns, with lower noise generally observed in northern and western Alaska and elevated noise in southern and coastal regions (Figure 8A).

The noisiest stations are concentrated in industrial, urban, sedimentary basin, and coastal settings. Of the 10% noisiest stations, eight are industrial, three are urban, nine are within sedimentary basins, and eleven are coastal or island sites. PS09 has the highest noise level overall. Several of these stations also occur in fjords or near glaciers, including BAE, BCP, and BGLC, while VMT combines a coastal fjord setting with nearby industrial infrastructure. Pipeline pump stations south of Fairbanks are generally noisier than pipeline sites north of Fairbanks, and RDOG at the Red Dog Mine complex in northwestern Alaska also exhibits elevated noise levels relative to nearby remote stations.

The 10% quietest stations are predominantly remote steel-cased boreholes installed in bedrock or fractured rock, with F18K as the only permafrost site. C21K has the lowest noise level in this period band.

4.3.2 1s period noise characteristics

The 1s band is associated with teleseismic body waves and regional seismicity (Ringler et al., 2024), but also includes noise from human activity, glacier calving, sea ice, and ocean waves (McNamara et al., 2019). Noise generally decreases with distance from the coast, with industrial pipeline sites as notable exceptions (Figure 8B). PS06 exhibits elevated noise across all components relative to nearby stations.

The 10% noisiest stations are concentrated near the coast, with three industrial, four urban, fourteen sedimentary basin, and eighteen coastal or island sites. BGLC has the highest noise overall. Several high-noise sites combine coastal exposure with industrial infrastructure, fjords, glaciers, or sedimentary basins.

The 10% quietest stations are predominantly remote steel-cased boreholes installed in bedrock or fractured rock. G27K has the lowest noise level in this band and is located on bedrock in northeastern Alaska near the Canadian border.

4.3.3 5s period noise characteristics

Noise at 5s corresponds to the secondary microseism, which is strongly influenced by ocean wave activity and seafloor interactions (Cessaro, 1994; Aster et al., 2008; McNamara et al., 2019; Ringler et al., 2024). Across the AGN, noise generally decreases with distance from the coast, although several southern pipeline sites are exceptions (Figure 8C).

The 10% noisiest stations are concentrated in coastal, island, and sedimentary basin settings: six are industrial, five are urban, seventeen within sedimentary basins, and seventeen are coastal or island sites. All stations in this group fall into at least one of these categories. R16K and CAPN rank among the highest noise stations, while BARK again represents an exception to the dominant site classifications.

The 10% quietest stations are predominantly remote boreholes installed in solid or fractured bedrock. E18K has the lowest noise level, although its estimate is based on less than 50% data availability; E24K is the next quietest site.

4.3.4 18s period noise characteristics

Noise at the 18s period band corresponds to the primary microseism band, commonly centered near 14s (Ringler et al., 2024; McNamara et al., 2019), and is generated by near-shore wave breaking and nonlinear interactions between ocean waves and the sloping seafloor (Hasselmann, 1963). Spatial noise patterns at this period are less coherent than in the secondary microseism band (Figure 8D), with elevated noise levels concentrated at island stations, throughout southeast Alaska, and within a cluster of stations in the Chugach-St. Elias Mountains.

Among the 10% noisiest stations, most are along the southern and southeastern coasts or in southcentral Alaska. Fifteen are coastal or island sites, eight are within sedimentary basins, three are industrial, two are urban. Twelve are installed in AEC-style vaults. The highest noise levels occur at R32K, a TA-style borehole installation. GOAT, which was converted from a vault to a borehole during the 2022 field season, and NIKH, which underwent a sensor replacement due to a faulty sensor, also rank among the noisiest stations, highlighting the influence of installation and instrumentation changes on observed noise levels.

In contrast, the 10% quietest stations are all borehole installations, predominantly on solid bedrock. Exceptions include three sites on fractured bedrock (A21K, E27K, G23K), and three in permafrost (A22K, C16K, F18K). Most are remote, with a few rural (D17K, E22K, H16K) and urban (A21K, TNA) sites. The quietest stations are distributed across the Brooks Range and the

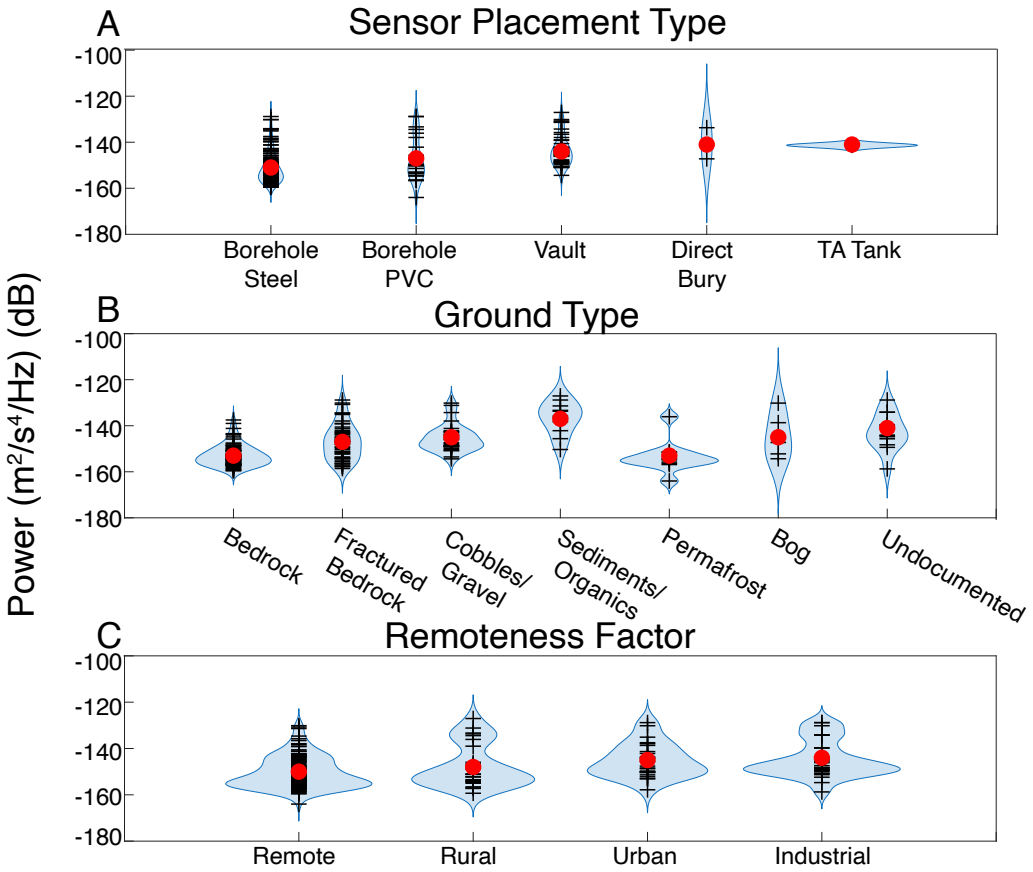

Figure 9 Power spectral density levels for all stations grouped by sensor placement type (A), ground type (B), and remoteness factor (C). Violin plots (blue) show the distribution of values within each category, with width proportional to data density. Black crosses indicate individual station values, and red circles denote the mean power for each group averaged across all channels and modes.

North Slope, with F15K, G17K, and H16K all tied for the lowest average noise level at -159.3 dB.

4.3.5 35s and 75s period noise characteristics

The 35s and 75s bands show similar spatial patterns and were therefore averaged when identifying the 10% quietest and noisiest stations. Vertical-component noise varies relatively little across the network, whereas horizontal components show higher noise levels and a general decrease with increasing latitude (Figure 8E-F). The noisiest stations are concentrated along the southern and southeastern coasts and in southcentral Alaska.

Among the 10% noisiest stations, six are industrial, three urban, seven within sedimentary basins, and twelve coastal or island sites. Approximately half are installed in AEC-style PVC vaults, with most of the remainder in steel-cased boreholes. R32K has the highest noise levels in this band. The 10% quietest stations are exclusively borehole installations, predominantly in solid bedrock; two are on permafrost, two in bog environments, and two on fractured bedrock. C27K has the lowest noise level overall.

4.4 Noise levels by remoteness, sensor emplacement, and ground type

We examined network-wide noise as a function of sensor emplacement, ground type, and remoteness using annual values averaged across all six period bands and three components (Figure 9, Table S5).

Overall trends were consistent with expectations. Among sensor placement types, steel-cased boreholes exhibit the lowest average noise levels, followed by PVC-cased boreholes and vaults, though some overlap exists, with a few boreholes noisier than some vaults (Figure 9A). The two remaining categories, direct bury and TA-style tank, have too few data points to be statistically significant, though the TA-style tank appears to provide a quieter environment than direct bury.

Noise levels varied with ground type, with bedrock sites exhibiting the lowest average noise, followed by permafrost and fractured rock (Figure 9B). Sites classified as cobbles/gravel were the fourth-lowest noise group out of seven, while stations located in sediments or organic-rich material had the highest average noise.

Remoteness also influenced observed noise. Remote sites had the lowest average noise, followed by rural sites, whereas industrial and urban sites had similar average noise levels, with industrial sites only slightly noisier than urban sites (Figure 9C). Across all factors, the quietest stations were installed in steel-cased boreholes on bedrock at remote locations (Figure S1).

4.5 Seasonal behavior

Seasonal variability was strongly dependent on period band and component (Figure 10). The largest and most

spatially coherent seasonal differences occurred in the 5 and 18s microseism bands, where horizontal noise was generally higher in winter. In contrast, vertical components and the long-period bands showed substantially less consistent seasonal behavior. Vertical components display greater station-to-station variability and no clear regional trend.

At the 0.2s period (anthropogenic band), the vertical components show little seasonal variation across most of the state, with exceptions in the Chugach-St. Elias region, the Aleutians, eastern Alaska near the Wrangell Mountains and eastern Alaska Range, and isolated sites in Interior and northern Alaska (Figure 10A). The horizontal components exhibit stronger seasonal variability, with coastal sites in the Chugach-St. Elias region generally noisier in winter, while higher-elevation mountain sites tend to be quieter in winter and noisier in summer. Wintertime increases are also observed at other coastal locations, including the Aleutians, Bering Sea, Prince William Sound, and the Arctic coast.

At 1s (teleseismic band), a southeast-to-northwest gradient is observed (Figure 10B). Stations in southeastern Alaska, southcentral Alaska, and the Aleutians are noisier in winter, whereas stations in northwestern Alaska, including Beaufort and Bering Sea coastal sites, are quieter in winter. A small number of stations deviate from this regional pattern, with substantially higher winter noise on both vertical and horizontal components.

The secondary microseism band (5s) exhibits consistently higher noise levels in winter (Kalenda et al., 2015), particularly on the horizontal components (Figure 10C). This band shows the largest seasonal contrast between horizontal and vertical components among all period bands. Nearly all stations exhibit increased wintertime noise on the horizontal components, with PS07 as the primary exception. Vertical components display greater station-to-station variability and no clear regional trend.

Seasonal behavior in the primary microseism band (18s) is broadly similar to that observed at 5s, with higher winter noise levels across much of the network, especially on the horizontal components (Figure 10D). A subset of stations in the St. Elias region exhibits lower winter noise on the horizontal components relative to summer.

At long periods (35s and 75s), vertical components show little seasonal change, with noise levels generally unchanged or slightly elevated in winter (Figure 10E-F). In contrast, horizontal components display highly variable seasonal behavior with no consistent statewide pattern. One observable regional trend is that many stations in the Chugach-St. Elias region exhibit lower noise levels in winter than in summer.

Several stations show extreme seasonal differences across multiple period bands due to known operational or mechanical issues, including loss of remote mass recentering (A19K), frost jacking of the borehole casing (H21K and H22K), physical damage to cables or instrumentation (P16K). Stations that underwent instrumentation changes during the analysis period (A22K, B20K, BARK, CHUM, GOAT, GRIN, J26L, L20K, MDM, NIKH, POKR, and PPLA) display mixed seasonal responses across period bands, sometimes influenced by whether post-installation data were included in winter months.

No systematic dependence on remoteness was observed; remote, rural, urban, and industrial sites exhibited similar seasonal behavior across all period bands (Figure S2). Seasonal patterns across ground types were broadly similar in the 0.2, 5, and 18s bands (Figure S3), although permafrost sites showed lower winter noise at 1s. At long periods, fractured bedrock and cobble/gravel sites tended to be quieter in winter, whereas permafrost sites showed the opposite pattern.

Sensor emplacement exhibits the strongest association with seasonal behavior (Figure S4). Borehole installations show minimal seasonal variation across the anthropogenic and long-period bands; whereas vault installations displayed distinct seasonal behavior at the 18s and long-period bands. Coastal and island stations tended to be noisier in winter, while higher-elevation mountain sites tended to be quieter in winter.

4.6 Mass recenter analysis

Of the high-gain broadband stations in the AGN, 188 were included in the mass recenter analysis because remote mass recenter commands were unavailable at the eleven pipeline sites and two sites equipped with Centaur dataloggers (Figure 5C). Of these, 121 had 12 or fewer mass recenters in 2024 and sufficient data availability and were classified as "best-performing" (Table S2). These stations are distributed statewide and span a range of sensor emplacement, ground type, and remoteness classifications.

Five stations were classified as "marginal-performing," with between thirteen and eighteen recenters and more than 50% uptime. Nineteen stations had more than nineteen recenters and were classified as "worst-performing"; thirteen were repeat offenders, having also ranked among the highest recentered stations in one or more years since 2021.

Several recurring site characteristics are observed among these stations. AEC-style vault installations at BARN, KTH, RKAV, SII, TGL, and VRDI, installed between 2004 and 2007, are located on exposed ridges or hilltops and do not reach competent bedrock; and instead rest in weathered or fractured rock. Many of these vaults protrude above the ground surface, and these sites exhibit instability during spring thaw and fall freeze periods.

Additional poorly performing stations include PVC-cased boreholes at H21K and M11K, emplaced in bedrock and permafrost, respectively, where field notes document frost jacking of the casing. For H21K, while the sensor is emplaced in bedrock, the material above it in which the PVC-casing is placed is documented as tundra. This site was installed in 2015, visited in 2017 and 2019 with no notes of frostjacking in the field documentation, but in 2024 was documented as "frostjacked 2-3 ft" by field staff, with the casing "tilted and wobbling in the wind", and the hut "sinking and tilting". M11K, which is documented as installed in a permafrost

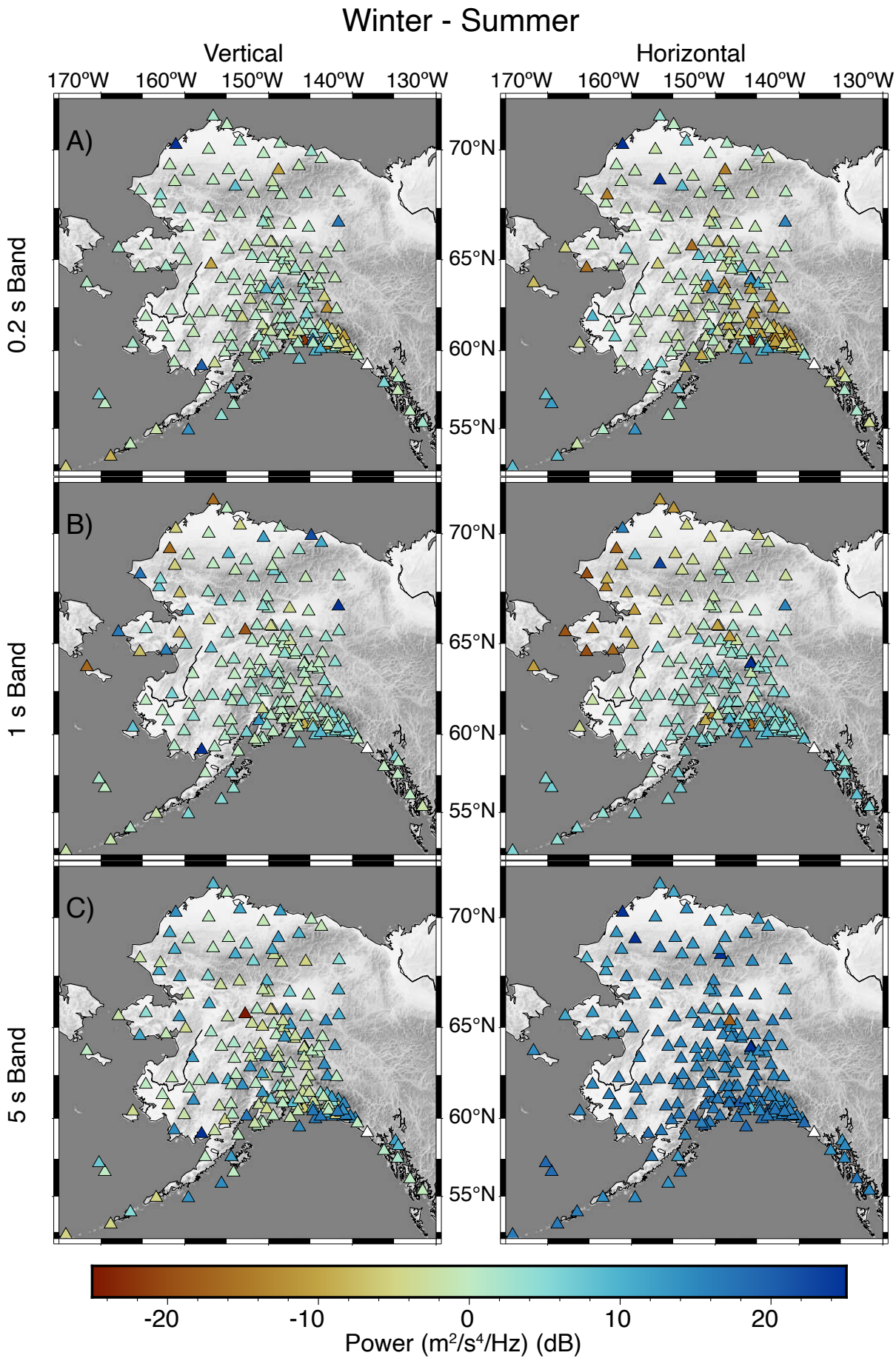

Figure 10 Side-by-side maps of winter minus summer differences for the 6 period bands for vertical (left panels) and an average of the two horizontal values (right panels). Negative values indicate a noisier summer and quieter winter. Positive values indicate a quieter summer and noisier winter. White values indicate no data for that station. A) 0.2s period band. B) 1s period band. C) 5s period band. D) 18s period band. E) 35s period band. F) 75s period band.

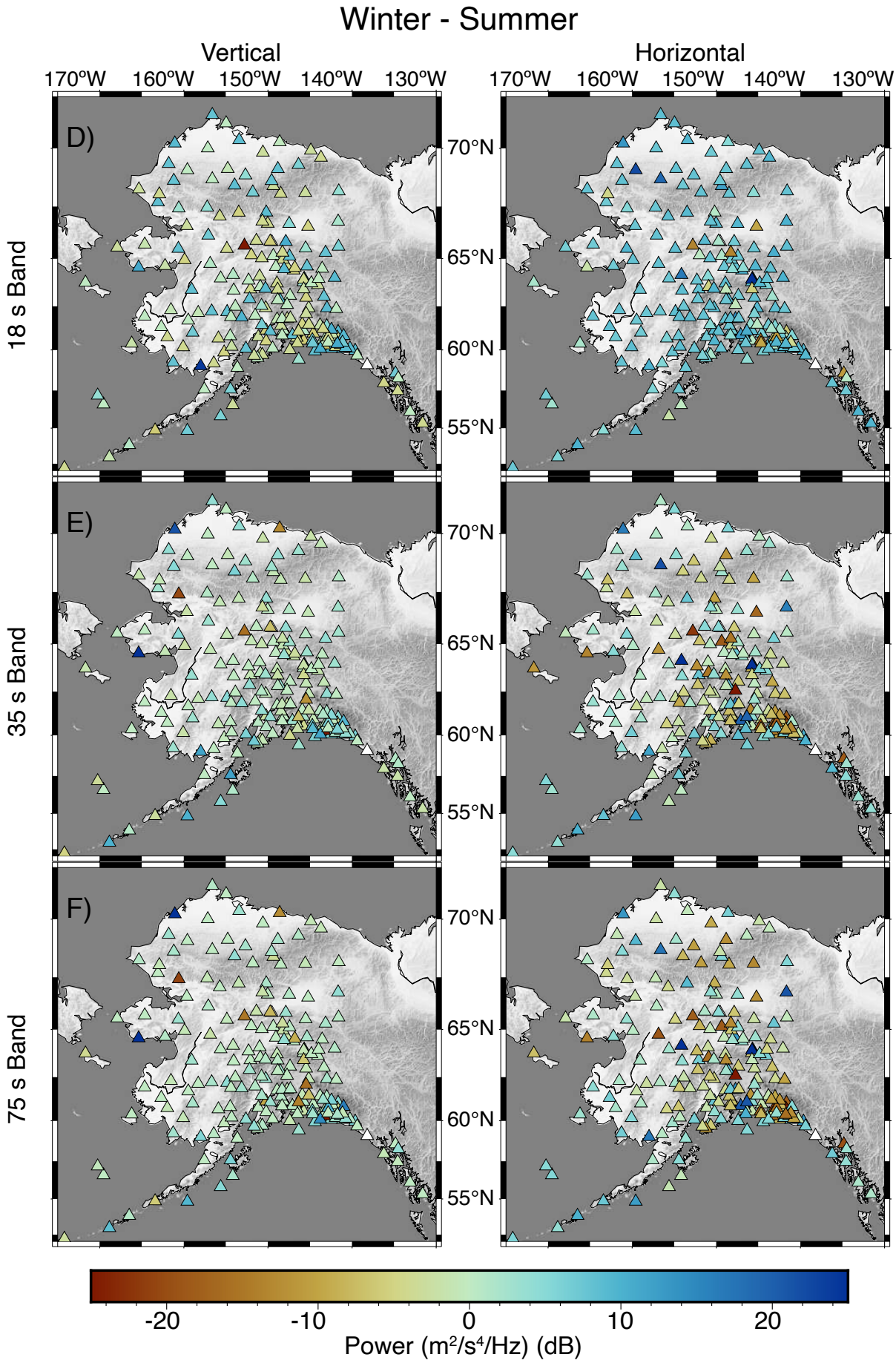

Figure 10 continued

environment, with "the water table just below the surface" in 2017, was not visited until 2021 and the casing was documented to be frostjacked 23 inches (during the 2026 field visit it was documented to be frostjacked 63 inches). Station R32K is a steel-cased borehole in a bog environment, with documented water intrusion into the cable conduit during the 2024 field season. This station is also at a ski lodge, where persistent cultural noise dominates the observed noise levels. M23K and P16K are steel-cased boreholes drilled into glacial moraines composed of fractured bedrock, cobbles, and soil. Stations I23K and Q19K are steel-cased boreholes that reached bedrock without evidence of permafrost; however, field notes indicate that the Q19K borehole was flooded, whereas I23K is located within dense vegetation with large tree roots near the borehole. The remaining 43 sites were assigned to the undetermined category because they lacked sufficient data for comprehensive analysis.

Because mass recenter activity can reflect either environmental instability or instrument malfunction, all known sensor and digitizer replacements during the study period (38 sites total; Table S2, "Site Information" sheet) were evaluated to help distinguish between these possible causes; the following stations underwent instrumentation changes during 2024. Digitizer replacements occurred at CHUM, L18K, L26K, MDM, and NEA2, while sensor replacements occurred at NIKH (STS-2A to T120), SAMH (T240 to new T240), and SSN (STS-5A to T120 PH). None of these stations were classified as "worst-performing", except SAMH, which recorded 151 recenters in 2024 (Table S2, "Mass Recenters" sheet, Table S3 "2024" sheet). SAMH went offline in April 2024, and following a field visit that restored telemetry and replaced the sensor, mass recentering activity ceased, suggesting the recenter activity at that site was instrument-related rather than environmentally driven.

5 Discussion

5.1 Anthropogenic and industrial noise sources

High-frequency seismic noise (0.2s band) is strongly influenced by anthropogenic and industrial activity, including mechanized traffic, industrial operations, and human presence near urban centers and sedimentary basins (Figures 8A and 10A). These signals are dominated by surface-wave propagation and attenuate over relatively short distances, so even modest distance from noise sources substantially reduces observed levels. Across the network, northern and western remote sites consistently exhibit lower noise levels, while southern coastal regions and areas near industrial or urban infrastructure show persistently elevated noise. Most pipeline sites, both north and south of Fairbanks, demonstrate particularly high noise (except PS04, discussed below), likely reflecting continuous mechanized operations that maintain elevated high-frequency noise year-round. However, the pipeline stations south of Fairbanks exhibit systematically higher noise levels than comparable sites further north, despite similar infrastructure types, indicating that regional environmental or geological setting modulates the expression of industrial noise. Seasonal trends (Figures 10A and S2) reinforce that these effects are stable across winter and summer, with only minor modulation from environmental factors.

Some industrial sites, however, behave more like remote locations, exhibiting lower noise levels than might be expected based solely on proximity to infrastructure. These quieter sites typically benefit from deeper borehole installation or shielding from local topography and surface structures, which reduces the impact of surface-wave propagation. For example, deep boreholes can isolate sensors from shallow anthropogenic vibrations, as suggested at PS04 in northern Alaska. However, interpretation of this site is limited because the sensor is malfunctioning and the horizontal channels are no longer recording ground motion. The RDOG mine site, despite industrial activity, shows noise levels comparable to remote stations. Although RDOG is a vault installation within cobbles, gravels, and fractured rock, the station's offset distance from anthropogenic activities (i.e. 2 miles from mining activity and 1 mile from significant human activity) contribute to RDOG's comparable noise levels to remote sites (Figures 8A and 10A). These observations underscore the importance of installation method, site geology, and distance from noise sources in mitigating high-frequency anthropogenic noise.

5.2 Effects of site geology and sedimentary basins

Seismic noise patterns clearly reflect the influence of basin structures and local geology across both high- and low-frequency bands (Figure 8). Sites within the Cook Inlet sedimentary basin consistently appear among the highest-noise stations in the network, not only in the anthropogenic band (0.2s), but also in the teleseismic and microseismic bands (1-18s). This recurring appearance indicates that sites within basins consistently exhibit higher noise levels across multiple bands. Elevated noise is observed both in coastal and inland basin sites, demonstrating that basin location alone does not fully explain these patterns.

Differences among bedrock, fractured rock, and unconsolidated sediments further illustrate the role of physical site coupling (Figures 7 and 9B). Solid bedrock sites generally exhibit lower noise levels. Fractured rock or mixed cobble/soil sites show moderate noise, while sediments, organics, and boggy materials show the highest noise. These patterns are consistent with differences in ground firmness and sensor coupling, rather than explicitly measured wave-propagation effects.

5.3 Coastal, glacial, and oceanic influences on noise

Seismic noise in the secondary and primary microseism bands (5s and 18s) is strongly influenced by proximity to the ocean, with coastal, island, and fjord sites consistently exhibiting elevated noise levels relative to inland

locations (Figure 8C-D). This pattern reflects the dominant role of ocean wave-generated microseisms, which propagate efficiently inland and affect both vertical and horizontal components. Sites located on shallow continental shelves, within fjords, or near exposed coastlines are particularly affected, although coastal proximity alone does not fully predict noise performance. Several coastal and island sites perform better than nearby shoreline stations, suggesting that differences in local site response, including near-surface geology, sediment thickness, and installation conditions, may affect the amplitude of the incoming microseism signal recorded at each station. Differences in emplacement depth and local site conditions can also affect the amplitude of the recorded wavefield, particularly for near-surface noise sources (Hutt et al., 2017). Although the primary microseism originates from distant sources and is expected to be relatively coherent over regional scales, local site response can amplify or attenuate the recorded signal without requiring substantial differences in the regional source. Within the Chugach-St. Elias region, seasonal behavior is spatially heterogeneous: coastal stations exhibit increased wintertime noise, whereas nearby higher-elevation mountain stations remain comparatively quiet during the same period. These differences may reflect increased storm activity or freeze-thaw processes near the coast, as well as a stabilizing influence of snowpack at higher elevations (Quigley and West, 2023). This pronounced seasonal contrast between horizontal and vertical components is consistent with global observations, where stronger Northern Hemisphere winter storms enhance ocean-wave interactions that generate secondary microseisms and increase coastal wave loading associated with the primary microseism.

Glacial-adjacent environments further complicate this pattern. Several sites located near actively moving or calving glaciers appear among the noisier stations in multiple period bands, including the anthropogenic (0.2s), teleseismic (1s), and microseismic bands (Figures 8A-D). Unlike ocean-generated microseisms, glacier-related noise is most evident during the summer months, when melting, cracking, and ice motion are more active, and is reduced during winter when glaciers are largely frozen. The presence of both coastal and glacial sources at some sites contributes to elevated noise across a broad range of periods, underscoring that combined environmental factors, rather than coastal proximity alone, govern noise characteristics at these stations.

5.4 Permafrost, freeze-thaw cycles, and sensor stability

Permafrost conditions exert complex and site-dependent controls on seismic station performance, reflecting variations in sensor emplacement relative to the active layer, intact permafrost, or thermally disturbed ground. Seasonal noise analysis indicates that freeze-thaw processes in the active layer, along with other environmental factors, influence noise levels across the 0.2-5s periods and at longer periods, particularly in the horizontal components (Figure 10). While most stations show higher winter noise in the secondary and primary microseism bands, some vault sites in the St. Elias region exhibit reduced winter noise relative to summer, consistent with increased vault stability when lower temperatures and snow cover reduce diurnal temperature fluctuations and wind-induced vibrations. Borehole installations, including both PVC- and steel-cased sites, display more variable seasonal behavior, with roughly half the sites exhibiting higher winter noise and half exhibiting higher summer noise (Figure S4), highlighting the role of sensor-ground coupling and local thermal environment in modulating seasonal noise.

Mass recentering records and site inspections further indicate that permafrost-affected installations can experience additional instability beyond seasonal noise variation. Borehole sites installed in permafrost, including H21K and M11K, experienced frost jacking of PVC casings due to freeze-thaw cycles in the active layer, resulting in sensor tilts that manifest as elevated long-period noise (Figure S5). Additionally, the heat output of broadband sensors over time may have local impacts to emplacement and operating conditions, which may cause permafrost thaw, contributing to ground tilt. As an example, a T120-PH3 seismometer uses about .23 W per day and thus output approximately the same amount of energy, mostly through heat. The older T120-PH1 sensor uses and outputs about .49W and 0.62W for the T240 (Nicholas Pelyk, Nanometrics, written pers. comm., Aug 13, 2026). Analysis of these effects is beyond the scope of this study. These observations are consistent with the known effects of soil expansion and contraction in the active layer above permafrost (Zhao, 2024), which can physically displace borehole casings and affect sensor alignment. Horizontal components are particularly sensitive to these displacements, explaining the observed increases in long-period noise at affected sites. Notably, several stations with frequent mass recenters are in ground containing permafrost, underscoring the importance of local thermal and mechanical conditions in long-term sensor performance.

Ground instability can also affect borehole installations in saturated or mechanically weak soils. For example, the TA-style borehole site R32K, located in wet, boggy terrain in southeast Alaska, exhibits elevated long-period horizontal noise and frequent mass recenters. This behavior illustrates how saturated ground conditions, combined with seasonal freeze-thaw processes can degrade data quality even in borehole deployments outside of continuous permafrost regions.

The combined seasonal noise and mass recenter observations suggest that monitoring networks in permafrost-influenced environments should prioritize installation strategies that reduce susceptibility to freeze-thaw movement. Vaults anchored in well-coupled, mechanically stable ground appear to provide more consistent long-term performance, whereas PVC-cased boreholes installed in permafrost-affected soils may require additional stabilization measures. Potential mitigation approaches include deeper casing emplacement, thermal insulation of the near-surface

column, or collocated soil temperature monitoring to better characterize seasonal ground behavior. Routine mass recenter monitoring and documenting frost-jacking effects can further improve long-term data quality. These observations demonstrate that sensor performance in permafrost regions is dynamic, strongly influenced by installation type, local thermal conditions, and seasonal ground dynamics, a mechanism rarely addressed in previous network studies.

5.5 Sensor housing, emplacement, and long-term performance

Sensor emplacement method is strongly associated with network noise performance (Figures 7, 9A, and S1). Across the AGN, steel-cased boreholes consistently outperform vault installations, with lower average noise levels across most period bands. PVC-cased boreholes are intermediate, while AEC-style and TA-style vaults show more variable behavior. Some overlap exists between the site types, and a few vaults perform as well as boreholes, particularly where vaults are well-coupled to bedrock or installed in protected locations. These results highlight that, beyond the nominal housing type, local installation conditions, including how well the sensor is coupled to the ground and its exposure to environmental conditions, are associated with differences in observed noise levels. A clear regional example of emplacement effects is provided by UNV, the only borehole station in the Aleutian chain. Despite its relatively shallow depth (10 ft), UNV consistently exhibits lower noise levels than nearby vault-based stations, demonstrating that even minimal borehole installation can offer performance advantages in high-energy coastal environments.

Our results also demonstrate that station performance cannot be fully characterized using a single broadband or annual-average noise metric. Several stations identified as among the quietest in network-wide averages do not consistently rank among the quietest when individual period bands are examined. This frequency-dependent behavior reflects differences in site coupling, installation stability, and environmental forcing across spectral ranges, and highlights the importance of evaluating station performance across multiple period bands when selecting benchmark stations or assessing installation effectiveness.

Sensor type and tilt tolerance also play an important role in long-term performance. Sites equipped with STS-5A sensors appear disproportionately in the "worst-performing" mass recenter category, suggesting these sensors may be less tolerant of subtle borehole tilts or vault shifts. While this pattern is consistent across multiple years and environments, it is interpreted cautiously: sensor susceptibility is a hypothesis supported by the observed clustering rather than a definitive causal conclusion. Other sensor types did not exhibit comparable sensitivity, emphasizing that both sensor design and emplacement interact to influence noise performance and maintenance requirements over time.

Taken together, the results indicate that seismic noise across the AGN is controlled by interacting installation, geologic, and environmental factors, with their relative importance varying by period band. Sensor emplacement and ground coupling emerge as the strongest network-wide controls, with steel-cased boreholes generally exhibiting the lowest noise levels and solid bedrock sites providing the most consistently quiet conditions. Environmental setting is an important additional control, with anthropogenic and industrial activity dominating at short periods and ocean- and glacier-related processes contributing substantially at intermediate periods. Local ground conditions and seasonal processes further regulate these effects, especially at longer periods where ground instability and sensor tilt become important. Finally, sensor type and instrument condition can strongly influence individual stations, as demonstrated by the relationship between frequent mass recentering and particular sensor types and known mechanical problems. These results demonstrate that no single site characteristic predicts station performance across all period bands; instead, long-term data quality reflects the interaction among installation, ground conditions, environmental conditions and processes, and sensor characteristics.

Interpretation of these network-wide patterns is subject to limitations in data completeness and in the information provided by PPSD-based metrics. Although stations with insufficient data were excluded and data from preceding years were incorporated where necessary to improve coverage, this approach improves temporal completeness at the expense of introducing some interannual variability into estimates initially intended to characterize 2024 conditions. In addition, PPSD mode values characterize the statistical distribution of seismic noise but do not identify the physical source of individual noise signals. Elevated noise may therefore reflect multiple contributing factors, including anthropogenic activity, environmental processes, site geology, installation conditions, or instrument behavior. The combination of PPSD metrics with station characteristics, seasonal behavior, and mass-recentering observations provides additional context for interpreting these patterns.

5.6 Implications for remote monitoring and maintenance prioritization

The combination of network-wide noise metrics and mass recentering behavior provides predictive insight into latent failure risks at AGN stations (Figure 6). Sites that consistently exhibit elevated noise levels, particularly when coupled with frequent mass recenter events, can be flagged for further evaluation of sensor or emplacement stability. This approach allows identification of sites that may not yet show catastrophic failure but require prioritized monitoring to prevent future performance loss. Because station performance may vary across spectral bands, maintenance prioritization and benchmark site selection benefit from evaluating noise behavior within specific frequency ranges relevant to monitoring objectives, rather than relying solely on broadband averages. Remote, rural, and industrial sites can all benefit from this combined evalua-

tion, highlighting that site isolation alone does not guarantee stability or low noise.

Mass position monitoring and recentering have also been used operationally in other large-scale seismic deployments, including the US Transportable Array (Busby et al., 2018). In the AGN, mass position is monitored operationally using sensor- and digitizer-specific thresholds, with an automated or manual recenter command issued when the mass position exceeds the allowable range. Beyond the immediate purpose of restoring the sensor mass to its nominal position, the frequency and success of recenter commands provide an additional indicator of station stability: occasional successful recenters, in which the mass positions return to zero or near-zero, are expected during normal operation, whereas repeated recenter commands or unsuccessful recenters, in which the mass positions do not return to zero or near-zero, can indicate developing sensor tilt, casing movement, or other site instability. Stations with persistently high recenter rates or repeated unsuccessful recenter commands can therefore be flagged for maintenance evaluation and, where appropriate, targeted sensor replacement with a more tilt-tolerant instrument. However, sensor replacement is unlikely to resolve instability caused by physical movement of the emplacement itself, such as frost jacking of a borehole casing. In these cases, remediation may require substantially more extensive and costly intervention, such as drilling a new borehole, making early identification of recurrent mass-recentering behavior particularly useful for maintenance prioritization.

Operationally, the results inform a targeted maintenance strategy. Recommendations include replacing tilt-sensitive sensors at sites prone to frequent mass recenters, monitoring permafrost-adjacent installations for freeze-thaw-related vault or casing shifts, and deploying temperature loggers or soil probes to better understand environmental stressors. Additionally, replacing vaults with steel-cased boreholes where feasible, ensuring robust bedrock coupling for all installations, and closely documenting unusual seasonal behaviors will support long-term network reliability. These measures translate the observed patterns into actionable interventions that can optimize resource allocation for maintenance and site upgrades across the AGN.

6 Conclusions

We performed a systematic analysis of background seismic noise across Alaska Geophysical Network stations spanning January 2021- December 2024. Noise levels vary substantially across the network, both geographically and seasonally. Stations located along the southern and southeastern Alaska coastline, the Aleutian Arc, and on islands consistently exhibit the highest noise levels, while the quietest stations are concentrated in the Brooks Range and northern Alaska. These low-noise sites are almost exclusively remote borehole installations located in solid or fractured bedrock. The quietest site overall is E24K, a remote bedrock borehole station in northern Alaska, whereas the noisiest site is FALS, a coastal village station with a shallow vault installed in organics-rich soils. Although E24K exhibits the lowest average noise across all period bands and channels, D25K appears most consistently among the quietest stations when individual period bands are considered, ranking within the top 10% for all six analyzed bands. This distinction emphasizes that station performance depends on the frequency band of interest and reinforces the importance of multi-band evaluation when assessing site quality.

Seasonal behavior across the network is dominated by increased noise in the primary and secondary microseism bands during winter months, consistent with enhanced ocean wave activity. While this trend is widespread, stations installed in AEC-style vaults display more variable seasonal behavior than borehole installations. In some regions, particularly mountainous areas, vault sites exhibit lower winter noise relative to summer, highlighting the sensitivity of shallow installations to local environmental conditions. Seasonal noise variations show limited dependence on station remoteness. Remote, rural, urban, and industrial sites exhibit broadly similar seasonal patterns, indicating that natural environmental processes, particularly ocean-generated microseisms and freeze-thaw dynamics, are the dominant drivers of seasonal noise variability across Alaska, rather than local anthropogenic activity.

Station performance is strongly influenced by sensor emplacement and ground conditions. Steel-cased boreholes generally provide the lowest overall noise levels, followed by PVC-cased boreholes, with vault installations exhibiting the greatest variability. Sites installed in bedrock consistently outperform those located in sediments, organics, or boggy terrain. These results emphasize that local coupling conditions and installation methods play a critical role in determining long-term noise performance, often outweighing broader geographic or environmental factors.

Together, these findings demonstrate that seismic station performance in arctic and subarctic regions is fundamentally shaped by permafrost dynamics and installation-ground interactions. We show that sensor behavior in permafrost-influenced soils is not static: interactions between emplacement type, seasonal freeze-thaw cycles, and thermally disturbed ground, including ground modified by heat from the sensors themselves, produce measurable, site-specific effects on noise and mass recenter behavior. Some effects may be apparent within a single seasonal cycle, whereas progressive ground and emplacement changes may develop over multiple years, making their consequences particularly important for long-term monitoring networks, This distinction has practical implications for network design and deployment strategy: short-term deployments may adequately characterize seasonal noise behavior, but may not capture slower-developing installation-permafrost interactions that can affect sensor stability and maintenance requirements over the lifetime of a permanent station. This physical understanding underscores the importance of explicitly accounting for installation-permafrost interactions in network design, maintenance prioritization, and long-term mon-

itoring strategies. Rather than relying solely on generalized siting best practices, large regional networks in high-latitude environments benefit from emplacement strategies that anticipate freeze-thaw-driven coupling changes and evolving near-surface thermal conditions. Incorporating these considerations into deployment and maintenance planning will improve data quality and enhance long-term network resilience.

Acknowledgments

This project was made possible in part by USGS ANSS cooperative agreements G20AC00032, G24AC00003, and G25AC00536 and support from the Office of the Alaska State Seismologist. We thank the Alaska Earthquake Center staff and acknowledge that without their efforts to keep stations up and running and data acquisition constant, we would not have had sufficient data for this study. We would like to thank the reviewers (Dan McNamara, Dave Wilson, and the anonymous reviewer #2) for taking the time to read this manuscript and make suggestions. Any use of trade, firm, or product names is for descriptive purposes only and does not imply endorsement by the U.S. Government.

7 Data and code availability

All seismic power density function data were downloaded through EarthScope Consortium Web Services (https://service.earthscope.edu/), which were calculated from data provided by the AK seismic network (Alaska Earthquake Center, Univ. of Alaska Fairbanks, 1987). Mass recenter data, which is not publicly available through the EarthScope Consortium, has been saved as an Excel Workbook in Table S3.

8 Competing interests

The authors have no competing interests.

References

Aderhold, K., Anderson, K. E., Reusch, A. M., Pfeifer, M. C., Aster, R. C., and Parker, T. Data Quality of Collocated Portable Broadband Seismometers Using Direct Burial and Vault Emplacement. *Bulletin of the Seismological Society of America*, 105(5), 2015. doi: 10.1785/0120140352.

Agency, U. S. E. P. United States Environmental Protection Agency, 2022. https://www.epa.gov/climate-indicators/climate-change-indicators-permafrost. Retrieved January 23, 2025, from.

Alaska Division of Geological and Geophysical Surveys. Map showing sedimentary basins of onshore and continental shelf areas, Alaska., 2020. https://dggs.alaska.gov/pubs/id/12926. Accessed 4 February 2026.

Alaska Earthquake Center, Univ. of Alaska Fairbanks. Alaska Geophysical Network, 1987. doi: 10.7914/SN/AK.

Anthony, R. E., Ringler, A. T., and Wilson, D. C. Seismic Background Noise Levels across the Continental United States from USArray Transportable Array: The Influence of Geology and Geography. *Bulletin of the Seismological Society of America*, 112(2):646–668, Jan. 2022. doi: 10.1785/0120210176.

Aster, R. C., McNamara, D. E., and Bromirski, P. D. Multidecadal Climate-induced Variability in Microseisms. *Seismological Research Letters*, 79(2):194–202, Mar. 2008. doi: 10.1785/gssrl.79.2.194.

Berger, J., Davis, P., and Ekström, G. Ambient Earth noise: A survey of the Global Seismographic Network. *Journal of Geophysical Research: Solid Earth*, 109(B11), Nov. 2004. doi: 10.1029/2004jb003408.

Busby, R., Woodward, R., Hafner, K., Vernon, F., and Frassetto, A. The Design and Implementation of EarthScope's USArray Transportable Array in the Conterminous United States and Southern Canada. 2018. doi: 10.5281/ZENODO.3758248.

Busby, R. W. and Aderhold, K. The Alaska Transportable Array: As Built. *Seismological Research Letters*, 91(6):3017–3027, 2020. doi: 10.1785/0220200154.

Casey, R., Templeton, M. E., Sharer, G., Keyson, L., Weertman, B. R., and Ahern, T. Assuring the Quality of IRIS Data with MUSTANG. *Seismological Research Letters*, 89(2A):630–639, Feb. 2018. doi: 10.1785/0220170191.

Cessaro, R. K. Sources of primary and secondary microseisms. *Bulletin of the Seismological Society of America*, 84(1):142–148, Feb. 1994. doi: 10.1785/bssa0840010142.

Dybing, S. N., Ringler, A. T., Wilson, D. C., and Anthony, R. E. Characteristics and Spatial Variability of Wind Noise on Near-Surface Broadband Seismometers. *Bulletin of the Seismological Society of America*, 109(3):1082–1098, Mar. 2019. doi: 10.1785/0120180227.

D'Alessandro, A. and Ruppert, N. A. Evaluation of Location Performance and Magnitude of Completeness of the Alaska Regional Seismic Network by the SNES Method. *Bulletin of the Seismological Society of America*, 102(5):2098–2115, Oct. 2012. doi: 10.1785/0120110199.

Freymueller, J. T. and West, M. E. EarthScope networks in Alaska and northwestern Canada, Nov. 2024. doi: 10.1002/9781394195947.ch1.

Hasselmann, K. A statistical analysis of the generation of microseisms. *Reviews of Geophysics*, 1(2):177–210, May 1963. doi: 10.1029/rg001i002p00177.

Hutt, C. R., Ringler, A. T., and Gee, L. S. Broadband Seismic Noise Attenuation versus Depth at the Albuquerque Seismological Laboratory. *Bulletin of the Seismological Society of America*, 107(3): 1402–1412, Mar. 2017. doi: 10.1785/0120160187.

John, S. and West, M. E. Appropriateness of the McNamara and Buland's (2004) methodology for computing frequency-dependent seismic power, 2024. doi: 10.48550/ARXIV.2410.14071.

Johnson, C. W., Meng, H., Vernon, F., and Ben-Zion, Y. Characteristics of Ground Motion Generated by Wind Interaction With Trees, Structures, and Other Surface Obstacles. *Journal of Geophysical Research: Solid Earth*, 124(8):8519–8539, Aug. 2019. doi: 10.1029/2018jb017151.

Kalenda, P., Wandrol, I., Holub, K., and Rušajová, J. The Possible Explanation for Secondary Microseisms Seasonal and Annual Variations. *Terrestrial, Atmospheric and Oceanic Sciences*, 26(2-1):103, 2015. doi: 10.3319/tao.2014.10.15.01(t).

Kirschner, C. Map showing sedimentary basins of onshore and continental shelf areas, Alaska. *United States Geological Survey Miscellaneous Investigations Series Map*, (eet, scale 1:2,500,000), 1988.

McNamara, D. and Buland, R. Ambient Noise Levels in the Continental United States. *Bulletin of the Seismological Society of America*, 94(4):1517–1527, Aug. 2004. doi: 10.1785/012003001.

McNamara, D., Buland, R., Benz, H., and Leith, W. *An assess-*

ment of seismic noise levels for the Advanced National Seismic System backbone network and selected regional broadband stations. 2005. doi: 10.3133/ofr20051077.

McNamara, D., Boaz, R., Nakata, N., Gualtieri, L., and Fichtner, A. *Visualization of the seismic ambient noise spectrum*, page 1–29. Cambridge University Press, Apr. 2019. doi: 10.1017/9781108264808.003.

Peterson, J. R. *Observations and modeling of seismic background noise*. 1993. doi: 10.3133/ofr93322.

Quigley, C. A. and West, M. E. The Seismic Record of Wind in Alaska. *Bulletin of the Seismological Society of America*, 114(2):613–626, Oct. 2023. doi: 10.1785/0120230097.

Ringler, A. T., Aderhold, K., Anthony, R. E., Busby, R. W., Frassetto, A., Tanimoto, T., and Wilson, D. C. Perspectives on Transportable Array Alaska Background Noise Levels, Nov. 2024. doi: 10.1002/9781394195947.ch2.

Rohde, M. D., Ringler, A. T., Hutt, C. R., Wilson, D. C., Holland, A. A., Sandoval, L. D., and Storm, T. Characterizing Local Variability in Long-Period Horizontal Tilt Noise. *Seismological Research Letters*, 88(3):822–830, Mar. 2017. doi: 10.1785/0220160193.

Ruppert, N. A. and West, M. E. The Impact of USArray on Earthquake Monitoring in Alaska. *Seismological Research Letters*, 91 (2A):601–610, Oct. 2019. doi: 10.1785/0220190227.

Smith, K. and Tape, C. Seismic Noise in Central Alaska and Influences From Rivers, Wind, and Sedimentary Basins. *Journal of Geophysical Research: Solid Earth*, 124(11):11678–11704, Nov. 2019a. doi: 10.1029/2019jb017695.

Smith, K. and Tape, C. Seismic Response of Cook Inlet Sedimentary Basin, Southern Alaska. *Seismological Research Letters*, 91(1): 33–55, Oct. 2019b. doi: 10.1785/0220190205.

Smith, K., Tape, C., and Tsai, V. C. Seismic Response of Nenana Sedimentary Basin, Central Alaska. *Bulletin of the Seismological Society of America*, 113(2):762–781, Dec. 2022. doi: 10.1785/0120220160.

Tsai, V. C. and McNamara, D. E. Quantifying the influence of sea ice on ocean microseism using observations from the Bering Sea, Alaska. *Geophysical Research Letters*, 38(22), Nov. 2011. doi: 10.1029/2011gl049791.

Zhao, Y. Seismic site response, liquefaction-induced lateral spreading and impact of seasonal frost on pile foundations in cold regions [(Doctoral dissertation,], 2024.

The article *Seismic noise and data quality of broadband stations of the Alaska Geophysical Network* © 2026 by Heather McFarlin is licensed under CC BY 4.0.